Bulletin of Geophysics and Oceanography Vol. XX, n. X, pp. XXX-XXX; Xxxxx 20xx
DOI 10.4430/bgo00517

What mechanisms lead to the enhancement of sea surface chlorophyll-a in the Arafura Sea?

G. Napitupulu[1,2], M.R. Ramadhan[1], S. Nurdjaman[1,3], I.M. Radjawane[1,3,4], A.A. Lukman[5], A.Y. Yuliardi[6], M. Napitupulu[7] and S. Nurfitri[3]

[1] *Study Program of Oceanography, Bandung Institute of Technology, Cirebon, Indonesia*
[2] *Coastal Hazards and Energy System Science Laboratory, Hiroshima University, Hiroshima, Japan*
[3] *Research Group of Environmental and Applied Oceanography, Bandung, Indonesia*
[4] *Korea-Indonesia Marine Technology Cooperation Research Center, Cirebon, Indonesia*
[5] *Department of Oceanography, Diponegoro University, Semarang, Indonesia*
[6] *Department of Marine Science, Jenderal Soedirman University, Purwokerto, Indonesia*
[7] *Study Program of Shipbuilding Engineering, University of Indonesia, Depok, Indonesia*

(Received: 13 October 2024; accepted: 31 October 2025; published online: 6 March 2026)

ABSTRACT Sea surface clorophyll-a (SSC) represents a fundamental indicator of oceanic primary production and serves as a widely used proxy for phytoplankton biomass. Although upwelling is recognised as the dominant driver of SSC variability, precipitation and river discharge can substantially modulate its spatial and temporal distribution. This study examines the spatiotemporal dynamics of SSC in the Arafura Sea, utilising satellite-derived oceanographic data from 1998 to 2022, with a focus on the influences of upwelling, precipitation, and oceanographic conditions. Seasonal analysis reveals that SSC peaks during the SE monsoon (June-August), coinciding with intensified upwelling, as indicated by positive Ekman pumping velocity (EPV), reduced sea surface height, and lowered sea surface temperature (SST). Coastal regions consistently exhibit higher SSC, driven by riverine discharge and precipitation-enhanced nutrient input. Regional correlation analysis confirms that offshore EPV and increased precipitation are the dominant mechanisms driving SSC enhancement during the SE monsoon. Climatological correlation analysis further identifies a strong positive relationship between SSC and EPV in key regions, with a maximum correlation coefficient of 0.85. The spatial distribution of SSC exhibits a pronounced inshore-offshore gradient across both monsoon seasons, reflecting the interplay between coastal upwelling, stable river discharge, and nutrient runoff. The empirical orthogonal function analysis of interannual variability suggests that SSC fluctuations are influenced by additional drivers beyond the El-Niño Southern Oscillation, including SST co-variability and anomalous precipitation patterns over central and north-western Papua. These findings show that phytoplankton variability in the Arafura Sea is chiefly controlled by local ocean, atmosphere, and land interactions, underscoring their importance for ecosystem forecasting.

Key words: Arafura Sea, chlorophyll-a, rainfall, river discharge, upwelling.

1. Introduction

Sea surface clorophyll-a (SSC) serves as a fundamental indicator of oceanic biological and environmental processes, including primary productivity, fishery abundance, eutrophication, water quality, and ecosystem health (Napitupulu, 2024). As the primary photosynthetic pigment in phytoplankton, SSC is widely used as a proxy for phytoplankton biomass and plays a crucial role in understanding biogeochemical cycles and ocean-climate interactions (McCain *et al.*, 2006; Yuliardi *et al.*, 2025). The distribution and concentration of SSC are essential in shaping marine food webs, as phytoplankton serves as the base of the marine food chain (Napitupulu, 2025a). SSC can provide insights into the vertical structure of phytoplankton communities, with larger phytoplankton species dominating nutrient-rich environments, while smaller species thrive in oligotrophic conditions (Uitz *et al.*, 2006). These distinctions also underscore the importance of spatial resolution and ecological context when interpreting SSC patterns. Given its significance, understanding the mechanisms driving SSC variability is essential for assessing ocean productivity and ecosystem dynamics. Moreover, long-term SSC variability has been widely used as an early-warning indicator of ecosystem shifts and climate-driven changes in ocean productivity (Sinuraya *et al.*, 2023), particularly in tropical marginal seas where even small perturbations can cascade through the food web.

Phytoplankton contributes nearly half of the global primary production and plays a pivotal role in regulating oceanic carbon fluxes (Pierella-Karlusich *et al.*, 2020). Its growth and distribution are governed by multiple factors, including light availability, nutrient supply, and oceanic mixing processes (Napitupulu *et al.*, 2024a). Beyond its contribution to primary production, phytoplankton drives the oceanic biological carbon pump, sequestering atmospheric carbon dioxide into the deep ocean and, thereby, modulating global climate (Basu and Mackey, 2017). SSC concentration is a widely accepted proxy for phytoplankton biomass, being typically correlated with phytoplankton abundance. However, this correlation can vary due to differences in species composition, nutrient dynamics, and environmental conditions (Brewin *et al.*, 2019; Fernández-González *et al.*, 2022). For instance, the SSC-to-biomass ratio varies across phytoplankton taxa, with larger species generally exhibiting higher pigment concentrations in eutrophic waters, whereas smaller phytoplankton predominate in oligotrophic settings (Huot *et al.*, 2007; Gui and Sun, 2024).

One of the primary physical drivers of SSC variability is upwelling, a process that transports cold, nutrient-rich deep waters to the ocean surface, thereby stimulating phytoplankton growth (Napitupulu *et al.*, 2024b). Upwelling occurs in various oceanic regions, including coastal, equatorial, and open-ocean environments (Hidaka, 1972). Coastal upwelling, driven by wind stress and Ekman transport, is particularly significant, as it results in the offshore movement of surface waters, enabling deeper nutrient-laden waters to rise (Napitupulu *et al.*, 2022). This mechanism is not only seasonal but also sensitive to coastline geometry and atmospheric variability. Similarly, equatorial upwelling is influenced by the Coriolis force, where trade winds drive surface water divergence, leading to nutrient upwelling along the equator (Napitupulu *et al.*, 2025a). These processes enhance primary production and directly impact the distribution of SSC in the upper ocean. Understanding the timing and magnitude of upwelling is, therefore, essential for predicting seasonal blooms and their cascading effects on food-web dynamics (Nagi *et al.*, 2023).

Apart from upwelling, SSC variability is also influenced by freshwater inputs from precipitation and river discharge. Several studies have reported increased SSC concentrations following periods of heavy rainfall, primarily due to the introduction of terrestrial nutrients into the

marine environment (Huang *et al.*, 2011; Meng *et al.*, 2017; He *et al.*, 2024). In tropical shelf seas, western Borneo Island, extreme rainfall events can also enhance turbidity and reduce light penetration, producing nonlinear phytoplankton responses that complicate the interpretation of satellite-derived SSC signals (Radjawane *et al.*, 2024a). However, the relationship between rainfall and SSC is complex, as it depends not only on nutrient supply but also on the chemical composition of the precipitation itself, which can influence phytoplankton growth (Willey *et al.*, 1999). Temporal mismatches between rainfall events and biological response further complicate this relationship, particularly in regions with high hydrological variability (Khadami *et al.*, 2025). Additionally, riverine discharge plays a crucial role in modulating SSC by delivering freshwater plumes enriched with nutrients, altering water column stratification, and enhancing productivity in coastal and estuarine regions (Wang *et al.*, 2015; Babagolimatikolaei, 2024). River plumes are typically characterised by lower salinity, higher nutrient concentrations, and cooler temperatures, which significantly impact local oceanographic conditions and phytoplankton dynamics.

The Arafura Sea, located in eastern Indonesian waters, is a shallow continental shelf region bounded by the southern coast of Papua and the northern coast of Australia (Napitupulu, 2025b). This area, part of Indonesia's Fishery Management Area 718, is recognised for its high biological productivity and is often referred to as a "golden fishing ground" due to its abundant fish stocks (Resosudarmo *et al.*, 2009). The productivity of the Arafura Sea is closely linked to SSC concentrations, which support vital commercial fisheries, particularly for species such as mackerel and shrimp (Welliken *et al.*, 2018; Tirtadanu *et al.*, 2022; Ankam and Tarya, 2023). Despite its ecological importance, the Arafura Sea remains underrepresented in large-scale phytoplankton and ocean productivity studies compared to other tropical marginal seas. The region is strongly influenced by climate variability associated with monsoon winds and the El-Niño Southern Oscillation (ENSO) (Gustiantini *et al.*, 2018). Seasonal monsoon winds drive oceanographic processes in the Arafura Sea, with north-westerly winds prevailing from December to February and south-easterly winds dominating from June to September (Suryadarma *et al.*, 2023). These wind-driven processes play a crucial role in regulating upwelling intensity and nutrient availability, thereby influencing phytoplankton productivity (Nurfitri *et al.*, 2020). These unique characteristics highlight the need for region-specific investigations that capture both local forcing and climate-driven variability to better understand the mechanisms driving its high productivity.

The influence of terrestrial inputs on SSC in the Arafura Sea is particularly significant due to the presence of extensive estuaries along the southern coast of Papua. Riverine discharge from these estuaries introduces substantial nutrient fluxes, impacting SSC dynamics. Previous studies suggest that upwelling in the Arafura Sea is modulated by a combination of monsoonal forcing, oceanic currents, and ENSO-driven variability (Buton *et al.*, 2023). However, the precise mechanisms underlying phytoplankton blooms in this region remain poorly understood. Kämpf (2016) hypothesised that seasonal coastal upwelling occurs in the north-western Arafura Sea during June–November, driven by lee effects that generate negative sea level anomalies, facilitating onshore transport of deeper waters. Furthermore, Nezlin *et al.* (2012) highlighted the role of micronutrients, particularly iron, in regulating primary productivity. While previous studies have provided valuable insights, a comprehensive and spatiotemporally resolved understanding of how oceanographic parameters, such as sea surface temperature (SST), sea surface salinity (SSS), wind-driven upwelling, and precipitation, jointly modulate SSC in the Arafura Sea remains limited. Despite these findings, knowledge gaps persist regarding the spatial and temporal variability of SSC and its relationship with oceanographic and climatic drivers in the Arafura Sea. Addressing this gap is critical not only for advancing the fundamental understanding of shelf-sea

biogeochemistry but also for supporting the adaptive management of fisheries that rely on the timing and magnitude of primary production.

This study aims to analyse the variability of seven key oceanographic and meteorological parameters [SST, SSS, sea surface density (SSD), sea surface height (SSH), river discharge, Ekman pumping velocity (EPV), and precipitation] over the 1998–2022 period to investigate their influence on SSC dynamics in the Arafura Sea. This is the first study to integrate two decades of satellite observations and reanalysis products in a multivariate framework specifically targeting the Arafura Sea. This approach enables a multivariate assessment that captures both seasonal and interannual drivers influencing phytoplankton distribution. We hypothesise that the enhancement of SSC is primarily driven by river discharge, precipitation, and monsoonal forcing. Additionally, we assess the role of the ENSO in modulating interannual SSC variability. By elucidating the mechanisms governing SSC dynamics, this study contributes to a broader understanding of regional ocean productivity and its implications for fisheries and ecosystem management in the Arafura Sea.

2. Materials and methods

2.1. Data

This study focuses on the Arafura Sea, located between 3°–12.25° S and 130.75°–142.25° E (Fig. 1). The study area is further divided into six subregions, where regions A, B, and C are paired with regions D, E, and F, respectively. This division facilitates an analysis of the relationship between the spatially averaged 25-year (1998–2022) climatological mean of oceanographic variables within the designated control regions and the rainfall intensity in the corresponding terrestrial areas. Such a spatial framework is essential to disentangle land and sea interactions and their role in modulating coastal biogeochemical dynamics.

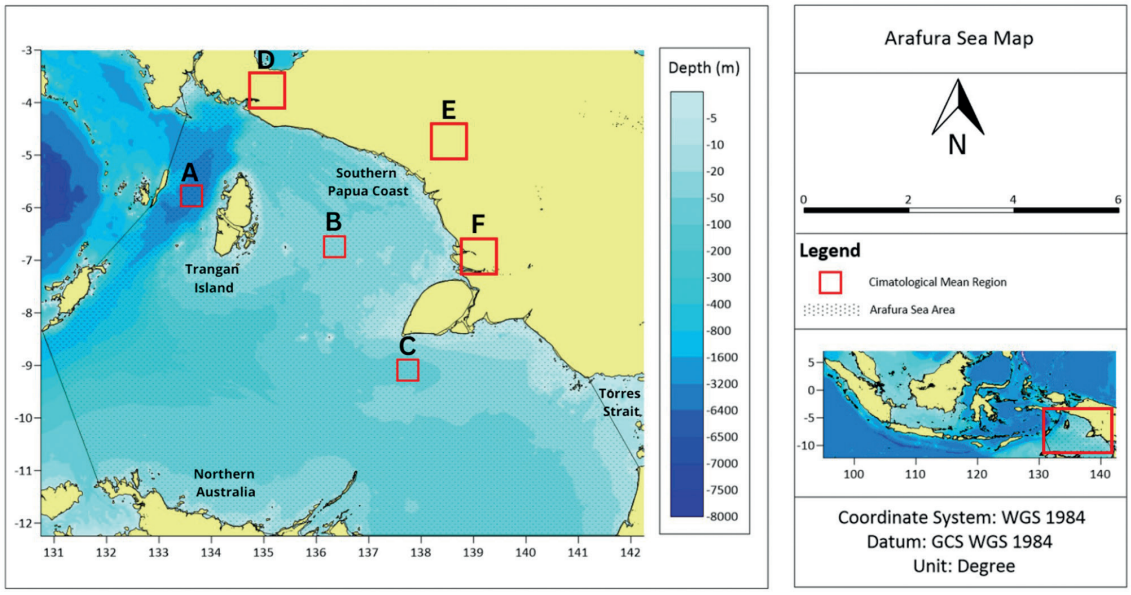

Fig. 1 - Research area (shaded black dot). The irregular shaded area represents the boundaries of the Arafura Sea, overlaid with a bathymetric map. The red rectangles denote the climatological data mean regions.

All oceanographic and meteorological variables were acquired from the Copernicus Marine Environment Monitoring Service (CMEMS) and the European Centre for Medium-Range Weather Forecasts reanalysis v5 (ERA5), which are proven to provide the necessary data with robust accuracy and reliability. Both CMEMS and ERA5 products undergo continuous validation and qualification processes to ensure their scientific robustness and consistency across time and space (von Schuckmann *et al.*, 2016; Le Traon *et al.*, 2019).

Satellite-derived daily SSC data were obtained at a spatial resolution of 4 km (Copernicus, 2024a). SST and SSH data were also retrieved from CMEMS for the same period (Copernicus, 2024b). River discharge data were obtained from CEMS-FLOODS for the same period (Copernicus, 2024c). In addition, sea surface wind (SSW) data at 10 m above sea level were obtained from ERA5 (Copernicus, 2018a). SSS and SSD datasets were retrieved from ERA5 (Copernicus, 2018b). All datasets were used to analyse oceanographic conditions in the Arafura Sea and their interactions with surrounding terrestrial systems.

Table 1 - Summary of the datasets used in this study.

Parameter	Source	Resolution	Period
Sea surface chlorophyll-a (SSC)	CMEMS	4 km × 4 km; daily	January 1998 – December 2022
Remote sensing reflectance (R_{rs}) 443	CMEMS	4 km × 4 km; daily	
Remote sensing reflectance (R_{rs}) 555	CMEMS	4 km × 4 km; daily	
Sea surface temperature (SST)	CMEMS	0.083° × 0.083°; monthly	
Sea surface height (SSH)	CMEMS	0.083° × 0.083°; monthly	
River discharge	CEMS-FLOODS	0.1° × 0.1°; daily	
Total precipitation	ERA5	0.1° × 0.1°; monthly	
Sea surface salinity (SSS)	ERA5	0.125° × 0.125°; monthly	
Sea surface density (SSD)	ERA5	0.125° × 0.125°; monthly	
Sea surface wind (SSW)	ERA5	0.125° × 0.125°; monthly	
Oceanic Niño Index (ONI)	NOAA	monthly	

Satellite-derived SSC values are often overestimated in coastal regions due to the influence of high suspended sediment concentrations and dissolved organic matter from riverine discharge (Napitupulu *et al.*, 2023; Quan and Chen, 2023). To address this bias, remote sensing reflectance (R_{rs}) data at 443 nm and 555 nm were used to differentiate upwelling and downwelling zones. Specifically, SSC values were considered unreliable in regions where $R_{rs}443$ exceeded 0.2 sr^{-1} or $R_{rs}555$ surpassed 2.5 sr^{-1} (Zhang *et al.*, 2022; Vos *et al.*, 2023).

2.2. Ekman pumping velocity

EPV quantifies the vertical movement of water masses driven by wind-induced divergence or convergence at the ocean surface. Upwelling occurs in regions where surface water diverges, transporting nutrient-rich waters from deeper layers to the surface, whereas downwelling is observed in areas of surface water convergence (Radjawane *et al.*, 2024b). Positive EPV values indicate upwelling, while negative values denote downwelling. This metric is particularly relevant in monsoon-dominated regions, where seasonal wind shifts exert strong control over vertical nutrient fluxes and phytoplankton productivity. Mathematically, EPV is defined as follows:

$$EPV = \frac{1}{\rho f} \nabla \cdot \tau \quad (1)$$

where ρ is the density of seawater, τ is the shear stress, and f is the Coriolis parameter, given by:

$$f = 2\Omega \cdot sin\varphi \quad (2)$$

where Ω is Earth's rotational speed and φ is latitude. This formulation enables the quantification of wind-driven vertical water transport, which plays a crucial role in determining SSC variability by influencing nutrient availability in the upper ocean.

2.3. Empirical orthogonal function analysis

The empirical orthogonal function (*EOF*) analysis was employed to identify dominant spatiotemporal variability modes in SSC, SST, and total precipitation (Napitupulu *et al.*, 2024c; Fathurohman *et al.*, 2025). This method decomposes datasets into orthogonal spatial patterns (the *EOF*s) and corresponding temporal components, i.e. principal components (*PC*s), enabling the identification of key oceanographic processes modulating SSC dynamics.

The *EOF* analysis is initiated by arranging the dataset in a matrix of dimensions $T \times S$, where T represents the temporal observations (rows) and S corresponds to the spatial points (columns). The temporal mean is subtracted at each spatial location to construct an anomaly matrix, from which a covariance matrix is computed:

$$Z'(x,y,t) = Z(x,y,t) - \overline{Z(x,y)} \quad (3)$$

$$S_{ij} = \frac{1}{T}\sum_{t=1}^{T} Z_i'(t) Z_j'(t) \quad (4)$$

where $Z'(x,y,t)$ is the anomaly of the observed variable and $\overline{Z(x,y)}$ is its temporal mean. The original dataset can, then, be reconstructed using the *EOF* decomposition:

$$Z(x,y,t) = \sum_{k=1}^{N} PC_k(t) \cdot EOF(x,y) \quad (5)$$

where $Z(x,y,t)$ is the original dataset, $PC_k(t)$ represents the time-dependent coefficient, and $EOF(x,y)$ describes the spatial variability pattern associated with each mode k. The variance explained by each mode serves as an indicator of its contribution to SSC modulation, with higher-ranked modes representing more dominant variability patterns.

3. Results

3.1. Seasonal variability of sea surface chlorophyll-a

The seasonal variability of SSC in the Arafura Sea is primarily characterised by high concentrations along the southern coastline of Papua (Fig. 2). The highest mean SSC concentration occurs in July, while the lowest is observed in December. Seasonally, SSC concentrations during the NW monsoon (December–February), first inter-monsoon (March–May), SE monsoon (June–August), and second

inter-monsoon (September–November) are 0.91, 1.02, 1.29, and 1.01 mg m^{-3}, respectively. The highest SSC is recorded during the SE monsoon, while the lowest is observed in the NW monsoon. This pattern aligns with the influence of monsoon-driven upwelling, which enhances nutrient availability through Ekman transport (Susanto *et al.*, 2001; Utama *et al.*, 2017). This metric is particularly relevant in monsoon-dominated regions, where seasonal wind shifts exert strong control over vertical nutrient fluxes and phytoplankton productivity.

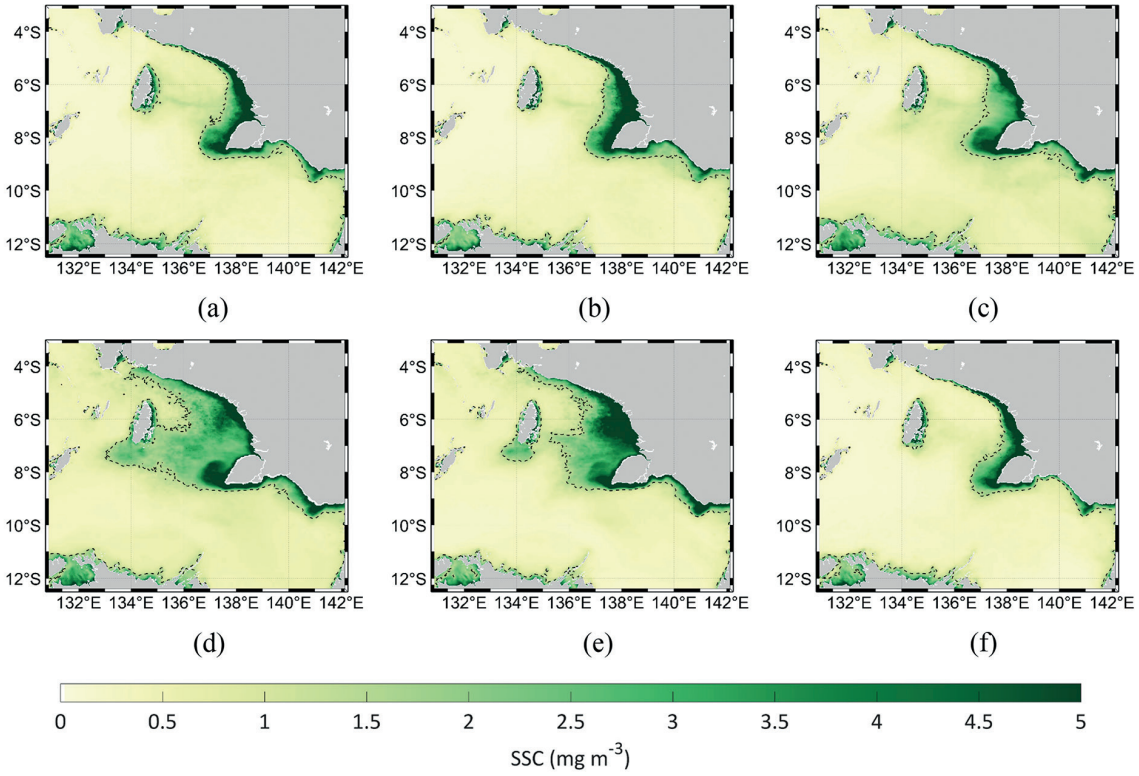

Fig. 2 - Monthly variation of SSC in the Arafura Sea in January (a), March (b), May (c), July (d), September (e), and December (f) from 1998 to 2022. Contour dashed line with value SSC 1.5 mg m^{-3}.

The relatively stable SSC concentrations along the coast may be attributed to persistent freshwater and nutrient inputs associated with high precipitation and river discharge, rather than enhanced vertical mixing. These inputs sustain phytoplankton growth through continuous nutrient supply despite increased surface stratification (Setiawan *et al.*, 2020). Additionally, continuous river discharge from estuarine environments supplies nutrients that sustain phytoplankton growth in the coastal areas. This persistent coastal productivity likely acts as a baseline ecological subsidy for nearshore ecosystems and fisheries. Offshore SSC enhancement can also result from mesoscale eddies (Correa-Ramirez *et al.*, 2007; Lukman *et al.*, 2024; Napitupulu, 2025c), particularly cyclonic eddies that induce localised upwelling. However, previous studies suggest that riverine nutrient transport can influence SSC levels up to hundreds or even thousands of kilometres from the river mouth (Auricht *et al.*, 2022). These findings imply that both local (e.g. river discharge) and remote (e.g. eddy-induced upwelling) mechanisms may synergistically modulate SSC dynamics across spatial scales in the Arafura Sea (Napitupulu, 2025b).

3.2. Seasonal variability of oceanographic and meteorological parameters

3.2.1 Seasonal variability of Ekman pumping velocity

EPV in the Arafura Sea exhibits significant seasonal variability, closely linked to monsoonal wind forcing. The highest positive EPV, associated with peak upwelling, is observed in July (~1.57×10^{-6} m s^{-1}), while the strongest downwelling occurs in February, marked by a negative EPV of -0.22×10^{-6} m s^{-1} (Fig. 3). Seasonally, the mean EPV values during the NW monsoon, first inter-monsoon, SE monsoon, and second inter-monsoon are -0.13×10^{-6}, 0.64×10^{-6}, 1.44×10^{-6}, and 0.32×10^{-6} m s^{-1}, respectively. The negative EPV values during the NW monsoon indicate downwelling conditions, whereas the positive EPV values during the SE monsoon are indicative of enhanced upwelling. This seasonal polarity in vertical motion aligns with observed SSC peaks during the SE monsoon, further emphasising the role of EPV as a primary physical driver of productivity.

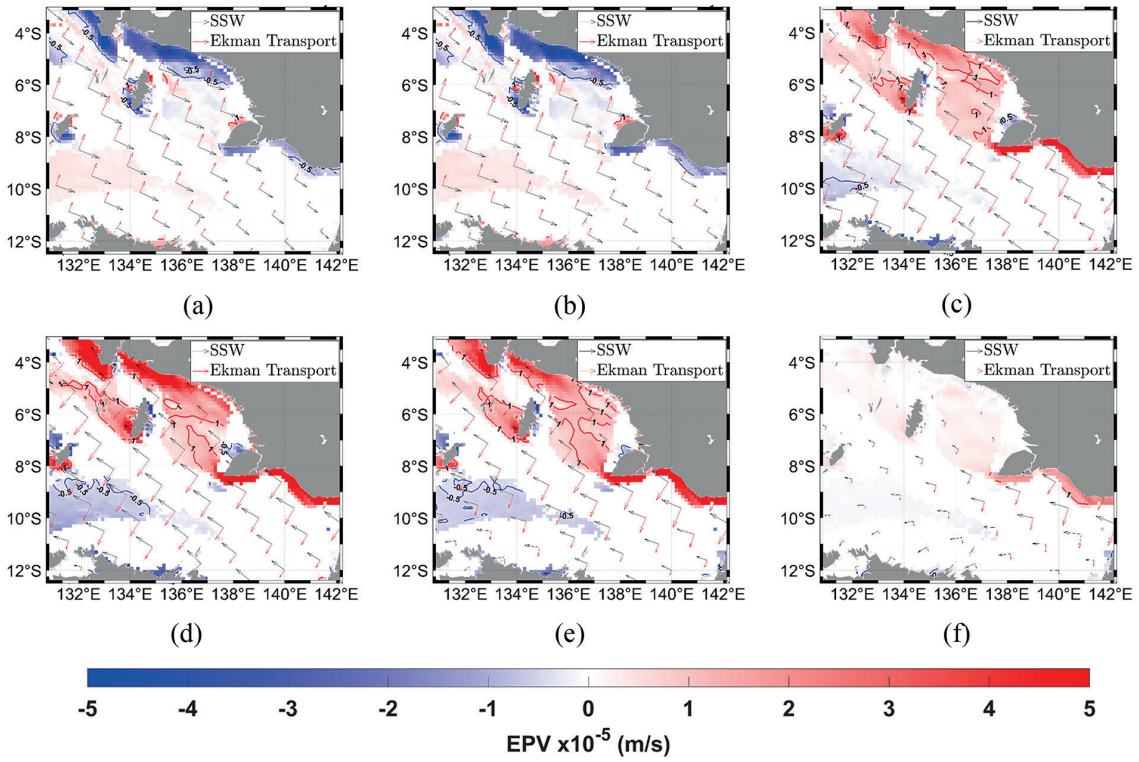

Fig. 3 - Monthly variation of EPV in the Arafura Sea in January (a), February (b), May (c), July (d), September (e), and November (f) from 1998 to 2022. Positive and negative values indicate upwelling and downwelling, respectively.

During the peak of the NW monsoon (January), significant downwelling is observed along the southern Papua coast near Trangan Island, in contrast to upward Ekman pumping in northern Australia. This downwelling is attributed to the weakening of south-easterly winds, which reduces offshore Ekman transport, leading to convergence and sinking of surface waters. In contrast, September marks the intensification of upwelling along the southern Papua coast and western

Trangan Island, as evidenced by positive EPV values. This progressive increase in EPV from May to September coincides with the onset of the SE monsoon, suggesting that phytoplankton blooms are likely initiated soon after sustained positive EPV anomalies are established (Napitupulu *et al.*, 2021). The spatial variability in Ekman transport across the Arafura Sea is influenced by coastline orientation, which modulates wind propagation and Ekman transport intensity (Gomez-Gesteira *et al.*, 2006; Bravo *et al.*, 2016).

During the peak of the second inter-monsoon (November), vertical water movement is generally weak due to reduced monsoon winds. However, localised upwelling is observed along the south-eastern coast of Papua, suggesting that regional coastal geomorphology and wind patterns contribute to sustained upwelling in this area. Collectively, these results indicate that EPV not only sets the seasonal bloom window but may also modulate its interannual amplitude, particularly during years of anomalously strong or weak monsoon winds.

3.2.2. Seasonal variability of sea surface height

Seasonal variations in SSH are closely associated with upwelling and downwelling processes. The seasonal mean SSH values during the NW monsoon, first inter-monsoon, SE monsoon, and second inter-monsoon are 0.79 m, 0.75 m, 0.61 m, and 0.68 m, respectively (Fig. 4). The highest SSH is recorded in December (0.81 m), while the lowest occurs in July (0.58 m). Elevated SSH during the NW monsoon is linked to downwelling, which deepens the thermocline and alters ecosystem dynamics (Gao *et al.*, 2019). Conversely, a decrease in SSH during the SE monsoon corresponds to an increase in SSC, highlighting the role of upwelling in bringing nutrient-rich waters to the surface.

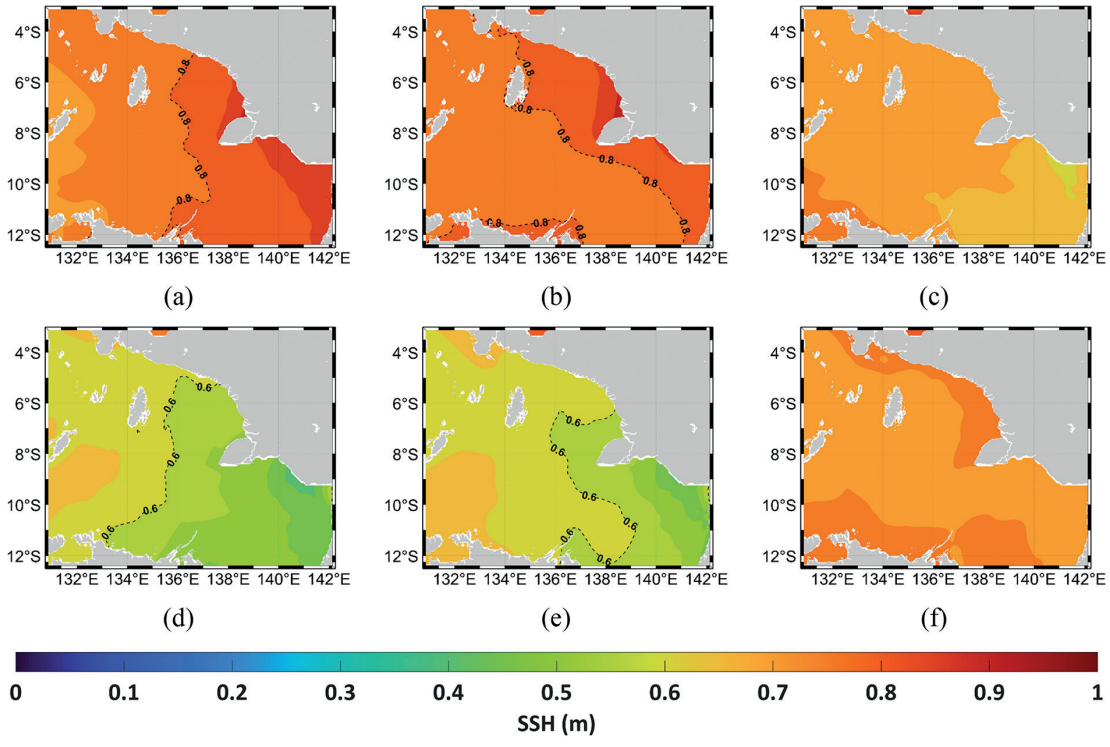

Fig. 4 - Monthly variation of SSH in the Arafura Sea in January (a), March (b), May (c), July (d), September (e), and November (f) from 1998 to 2022.

Low SSH reflects surface water divergence and the upward displacement of subsurface isopycnals, facilitating the entrainment of colder, nutrient-rich waters into the euphotic zone. Previous studies suggest that SSH variability in the Arafura Sea may be influenced by ENSO-driven atmospheric pressure fluctuations (Rahn, 2012). Additionally, Kelvin waves have been shown to modulate SSH and coastal upwelling by inducing vertical displacement of water masses (Wiafe and Nyadjro, 2015). These processes act as remote drivers of nutrient entrainment, superimposed on the local wind-driven upwelling signal, thereby introducing additional complexity to seasonal bloom prediction. Consequently, SSH can serve as a useful early-warning indicator for upwelling-driven productivity events in the Arafura Sea, particularly during the SE monsoon.

3.2.3. Seasonal variability of sea surface temperature

SST in the Arafura Sea exhibits clear seasonal variability, reflecting changes in atmospheric forcing and oceanic circulation. The seasonal mean SST values for the NW monsoon, first inter-monsoon, SE monsoon, and second inter-monsoon are 29.73 °C, 29.14 °C, 26.53 °C, and 27.99 °C, respectively. The highest monthly SST (30.05 °C) occurs in December, while the lowest (25.95 °C) is recorded in August (Fig. 5). Seasonal SST fluctuations align with SSC variations, supporting the role of SST as an indicator of upwelling dynamics (Arcos and Wilson, 1984; Napitupulu, 2025a). Seasonal precipitation variability alone does not explain the observed SSC patterns, indicating that physical processes such as upwelling and vertical mixing play a more dominant role.

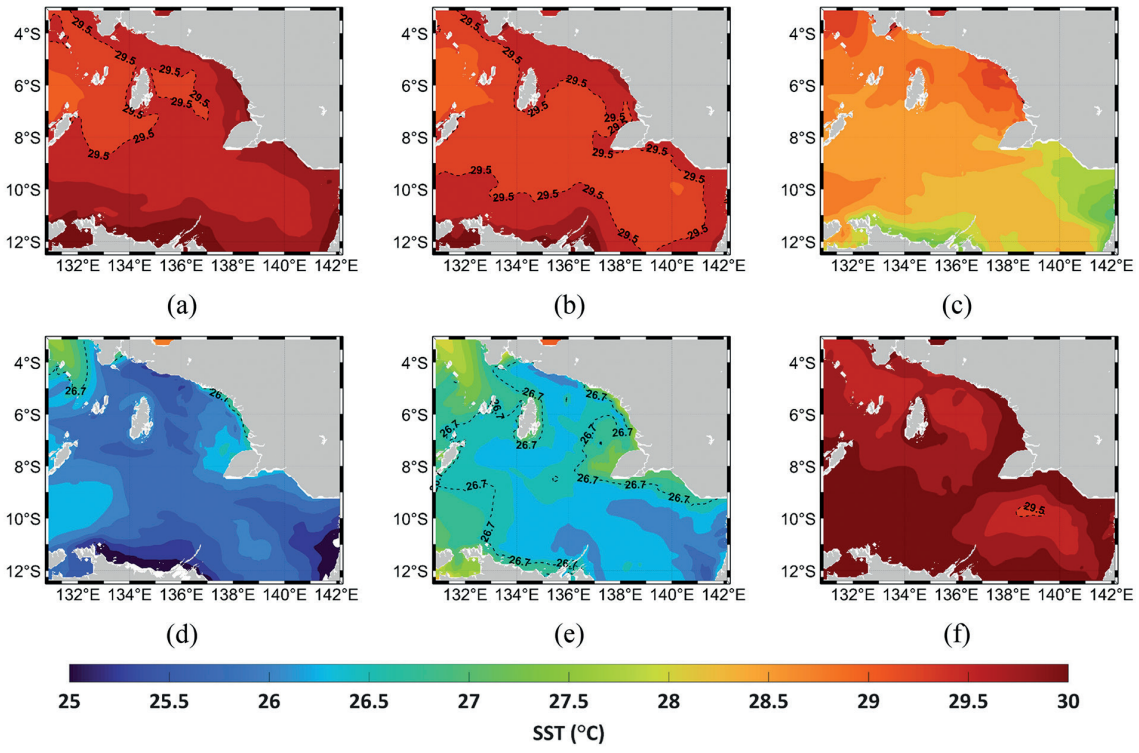

Fig. 5 - Monthly variation of SST in the Arafura Sea in January (a), March (b), May (c), August (d), September (e), and December (f) from 1998 to 2022.

3.2.4. Seasonal variability of total precipitation

Total precipitation in the Arafura Sea exhibits relatively weak seasonal variability, with mean values of 0.0128 m (NW monsoon), 0.0124 m (first inter-monsoon), 0.0089 m (SE monsoon), and 0.0099 m (second inter-monsoon) (Fig. 6). The SST minimum during the SE monsoon reinforces evidence of upwelling-induced surface cooling, concurrent with enhanced SSC and positive EPV.

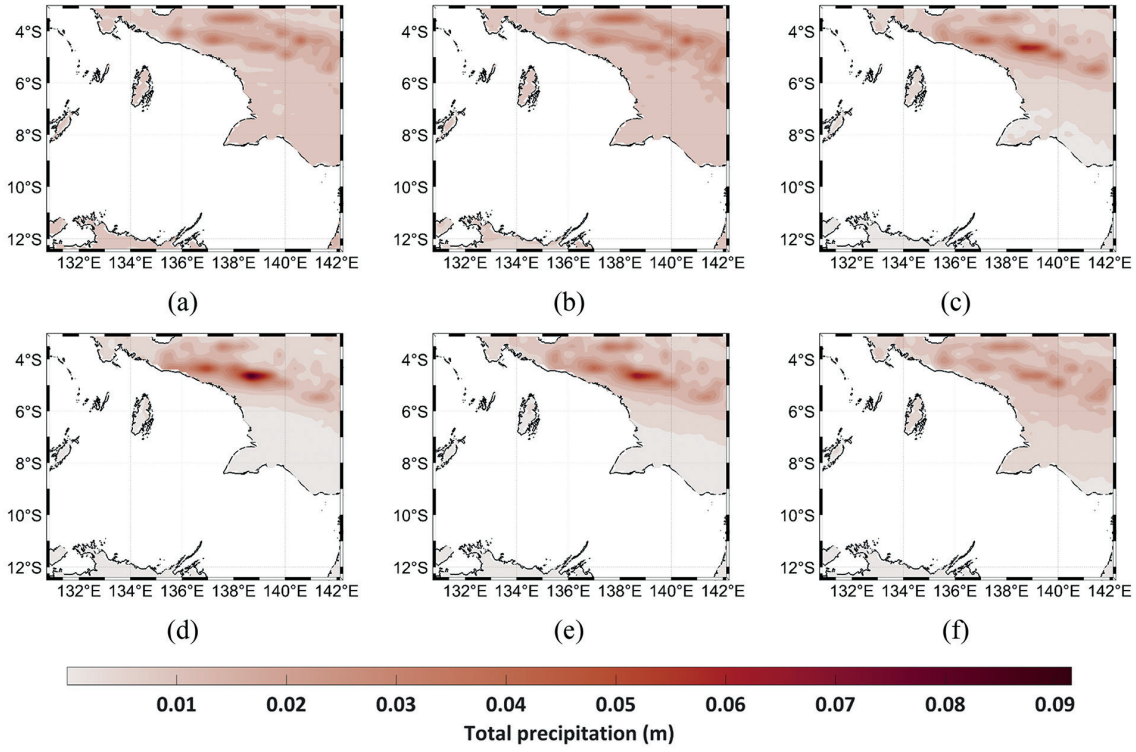

Fig. 6 - Monthly variation of total precipitation in the Arafura Sea in January (a), March (b), May (c), July (d), September (e), and November (f) from 1998 to 2022.

Seasonal precipitation patterns suggest that local convective processes and orographic effects over Papua Island exert a greater influence on rainfall variability than water vapour advection from northern Australia. Increased precipitation enhances freshwater discharge, reducing SSS and density while supplying nutrients that support phytoplankton growth (Meng *et al.*, 2017; Napitupulu *et al.*, 2023). However, precipitation alone does not fully explain SSC variability, as other factors, such as upwelling and seasonal mixing, contribute more significantly.

3.2.5. Seasonal variability of sea surface density

SSD exhibits minor seasonal fluctuations, with mean values of 1021.43 kg m^{-3} (NW monsoon), 1021.30 kg m^{-3} (first inter-monsoon), and 1021.39 kg m^{-3} for both the east and second inter-monsoons (Fig. 7). Although the amplitude of SSD variation is small, its spatial gradient may indicate subsurface water intrusion from offshore sources during upwelling episodes.

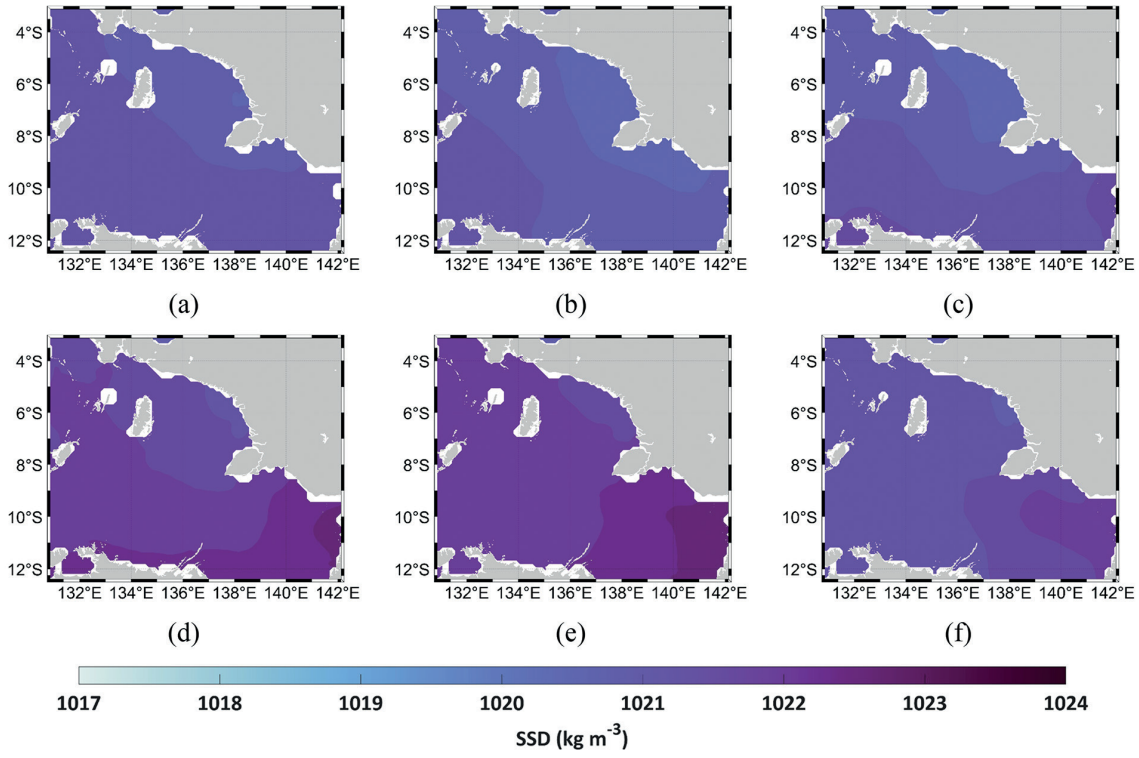

Fig. 7 - Monthly variability of SSD in Arafura watersin January (a), March (b), May (c), July (d), September (e), and November (f) from 1998 to 2022.

Higher SSD and SSS offshore suggest upwelling of subsurface water masses, which enhances nutrient availability and supports phytoplankton productivity (Hughes and Barton, 1974). The horizontal profile of SSD exhibits a gradual increase towards offshore regions, reflecting variations in vertical mixing and pycnocline depth. These factors influence nutrient entrainment, directly impacting phytoplankton growth (Kubryakova *et al.*, 2018).

However, SSD and SSS alone do not fully explain phytoplankton dynamics. Their influence must be considered alongside other parameters, such as EPV, SST, SSH, and direct SSC measurements. Integrating these oceanographic parameters with hydrodynamic modelling and *in-situ* nutrient observations would provide a more comprehensive understanding of phytoplankton bloom dynamics in the Arafura Sea.

3.2.6. Seasonal variability of sea surface salinity

SSS in the Arafura Sea shows minor seasonal changes (Fig. 8), with mean values of 33.89 ppt (NW monsoon), 33.88 ppt (first inter-monsoon), 33.87 ppt (SE monsoon), and 33.83 ppt (second inter-monsoon). January exhibits the highest surface salinity in northern Australia, while November records the lowest salinity levels (33.82 ppt). The distinct water mass characteristics between the southern Papua coast and northern Australia suggest the continuous influence of river plume discharge, modulating water mass transport in the Arafura Sea (Huisman *et al.*, 2006).

Salinity variations near the southern Papua coast are minimal due to persistent freshwater input from river discharge. However, seasonal changes in offshore salinity are more pronounced.

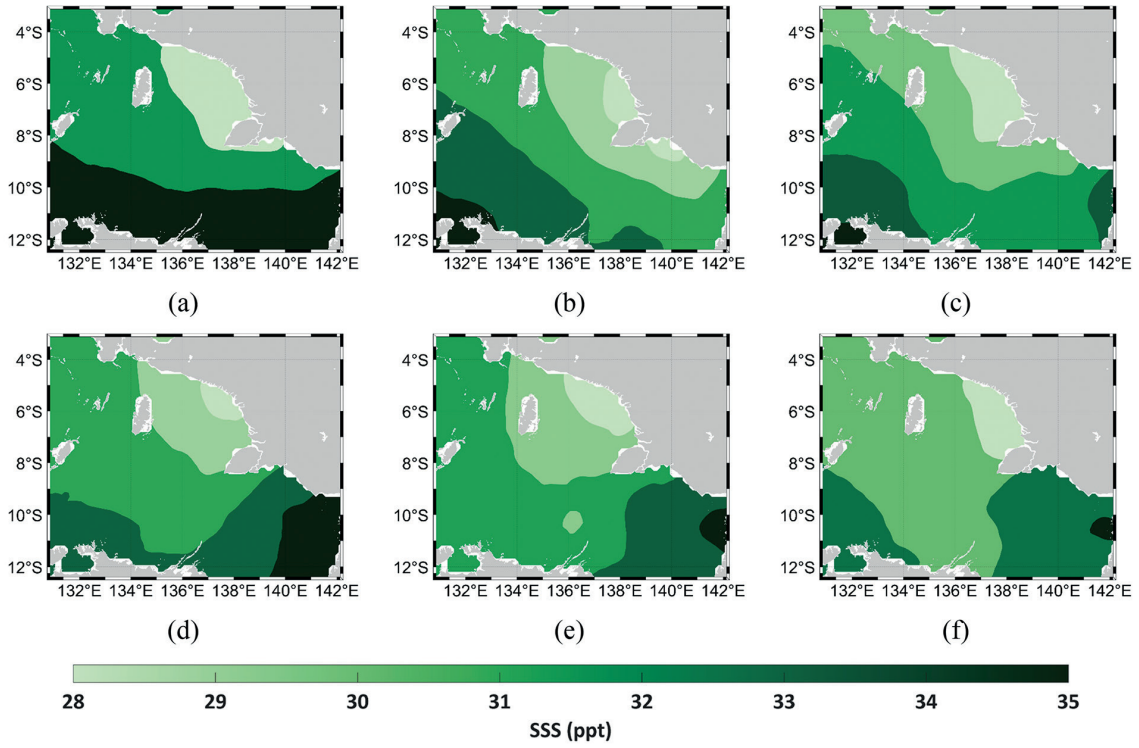

Fig. 8 - Monthly variability of SSS in Arafura waters in January (a), March (b), May (c), July (d), September (e), and November (f) from 1998 to 2022.

During January, negative EPV values coincide with widespread low-salinity water masses, while July, characterised by intense Ekman pumping, exhibits a relatively thin layer of low-salinity waters inshore. This pattern suggests that upwelling plays a more dominant role in modifying water mass characteristics compared to river runoff in this region.

3.2.7. Seasonal variability of river discharge

River discharge into the Arafura Sea shows a pronounced seasonal cycle, reflecting the strong influence of the monsoonal climate in Papua and northern Australia. During the wet season (November–March), intense rainfall drives high riverine fluxes of freshwater, sediments, and nutrients. These inputs freshen surface waters, increase turbidity, and enhance nutrient availability, stimulating primary productivity and sustaining fisheries. Local catchments, such as the Ajkwa River basin, also highlight the compounding role of anthropogenic activities, where mining accelerates sediment and pollutant delivery, intensifying ecological pressures during peak discharge (Ilahude *et al.*, 2024).

By contrast, the dry season (May–September) is characterised by minimal river inputs and clearer, saltier surface waters. Productivity during this period is, instead, sustained by coastal upwelling associated with the SE monsoon, which injects cooler, nutrient-rich waters from the Banda Sea into the Arafura shelf (Karima *et al.*, 2025). Although distinct in origin, the alternation between riverine forcing and oceanic upwelling produces a seasonal cycle that governs salinity, turbidity, and nutrient dynamics, ultimately driving variability in SSC across the region.

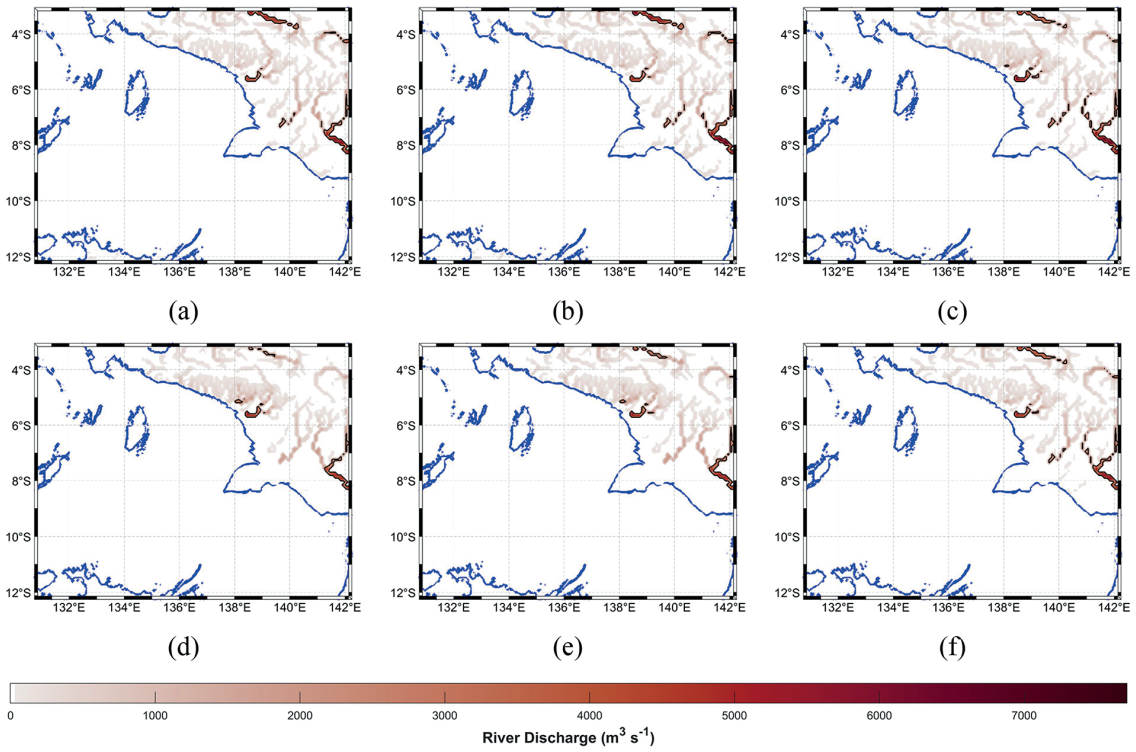

Fig. 9 - Monthly variability of river discharge in Arafura waters in January (a), March (b), May (c), July (d), September (e), and November (f) from 1998 to 2022.

3.3. Mechanism of increasing sea surface chlorophyll-a in the Arafura Sea

A regional analysis of the correlation between SSC and EPV reveals spatial variations (Fig. 10). In Region A, SSC and EPV exhibit a moderate negative correlation (r = -0.59), whereas in Region B and Region C, the correlation is strongly positive (r = 0.78 and r = 0.85, respectively). The positive correlation in Region B and Region C suggests that phytoplankton blooms are largely driven by wind-induced Ekman pumping, which enhances vertical nutrient supply during the SE monsoon. Conversely, the negative correlation in Region A may reflect the influence of coastal orientation, which modulates the magnitude and direction of Ekman pumping. This spatial heterogeneity underscores the importance of localised wind-topography interactions in shaping nutrient delivery pathways. Furthermore, SSC variability in Region B shows a strong positive correlation with total precipitation (r = 0.8), highlighting the role of freshwater influx in nutrient supply. This finding highlights the coupling between land–ocean interactions and monsoonal dynamics, suggesting that terrestrial nutrient fluxes may amplify bloom intensity when coincident with favourable wind-driven upwelling. Increased precipitation enhances river runoff, which can transport nutrients from terrestrial sources into the coastal ocean, fostering phytoplankton growth. The dual influence of wind-driven upwelling and terrestrial runoff in Region B suggests a synergistic mechanism enhancing primary productivity.

The correlation analysis between SST and SSH across all regions indicates a strong positive relationship, with r values of 0.94 (Region A), 0.97 (Region B), and 0.98 (Region C). Both variables exhibit a similar declining trend during the SE monsoon, suggesting the significance of upwelling in these regions. This synchronous decline supports the notion that surface cooling and sea level

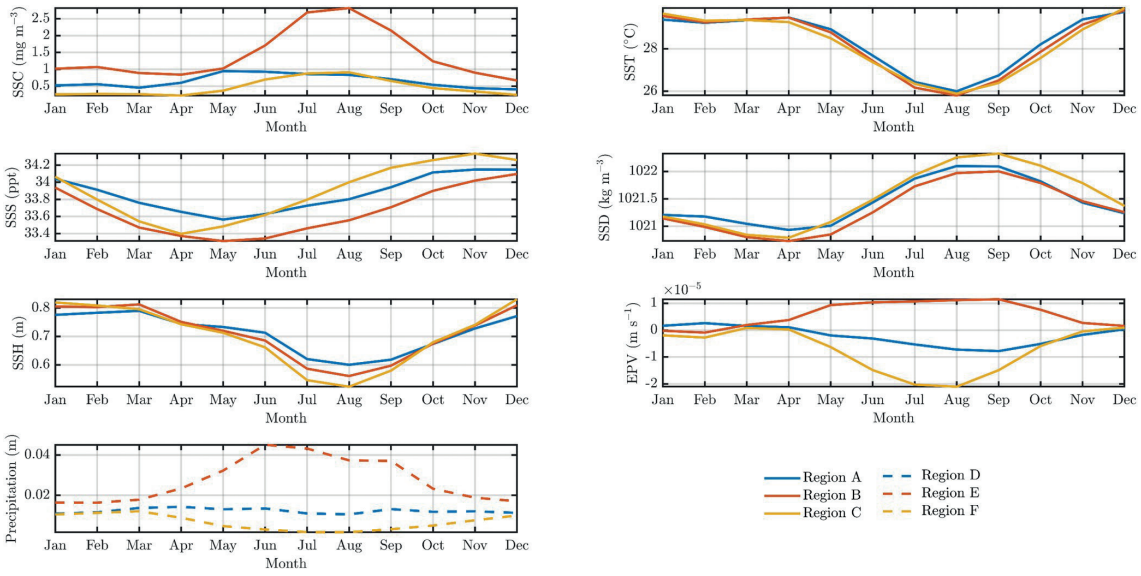

Fig. 10 - Regional monthly climatological mean of SSC, SST, SSS, SSD, SSH, EPV, and precipitation based on the region, which is Region A (a), Region B (b), and Region C (c) from 1998 to 2022.

drop are co-occurring indicators of upwelling-driven vertical exchange. This synchronised decline in SST and SSH during the SE monsoon indicates that wind-driven upwelling is the dominant control on their seasonal variability, while surface heat fluxes may play a secondary role in modulating SST (Meyssignac *et al.*, 2017).

Despite general similarities across regions, some differences in SSD and SSS dynamics are evident. In Region A and Region B, SSD and SSS decline in April and May, while in Region C, the lowest values are recorded in April. These differences indicate region-specific interactions between atmospheric forcing, ocean circulation, and freshwater input, which collectively regulate the distribution of SSC. Together, these results indicate that SSC enhancement in the Arafura Sea is governed by a nonlinear combination of local upwelling, freshwater nutrient input, and large-scale climate oscillations. This underscores the need for integrated monitoring that considers both atmospheric and oceanic drivers to predict productivity hotspots with higher accuracy.

3.4. Identification of surface chlorophyll-a dynamics factor based on net climatological changes

The climatological distribution of SSC indicates that elevated SSC values are primarily concentrated along the coastlines of surrounding islands, suggesting that river discharge, coastal upwelling, and precipitation are the dominant contributing factors. Inshore waters are characterised by reduced SSD and SSS, reflecting the influence of river plumes and freshwater dilution from precipitation (Fig. 11). In contrast, relatively high SST and SSH values along the coast suggest the dominance of downwelling processes during certain periods. Although total precipitation remains relatively uniform throughout the year, north-western and inland Papua experience higher rainfall intensities, which likely enhance SSC in the north-western Arafura Sea.

During the peak of the SE monsoon in August, a pronounced gradient in SSC between coastal and offshore waters reflects the intensification of coastal upwelling. This gradient highlights the combined effects of continuous river discharge, precipitation-driven nutrient input, and seasonal

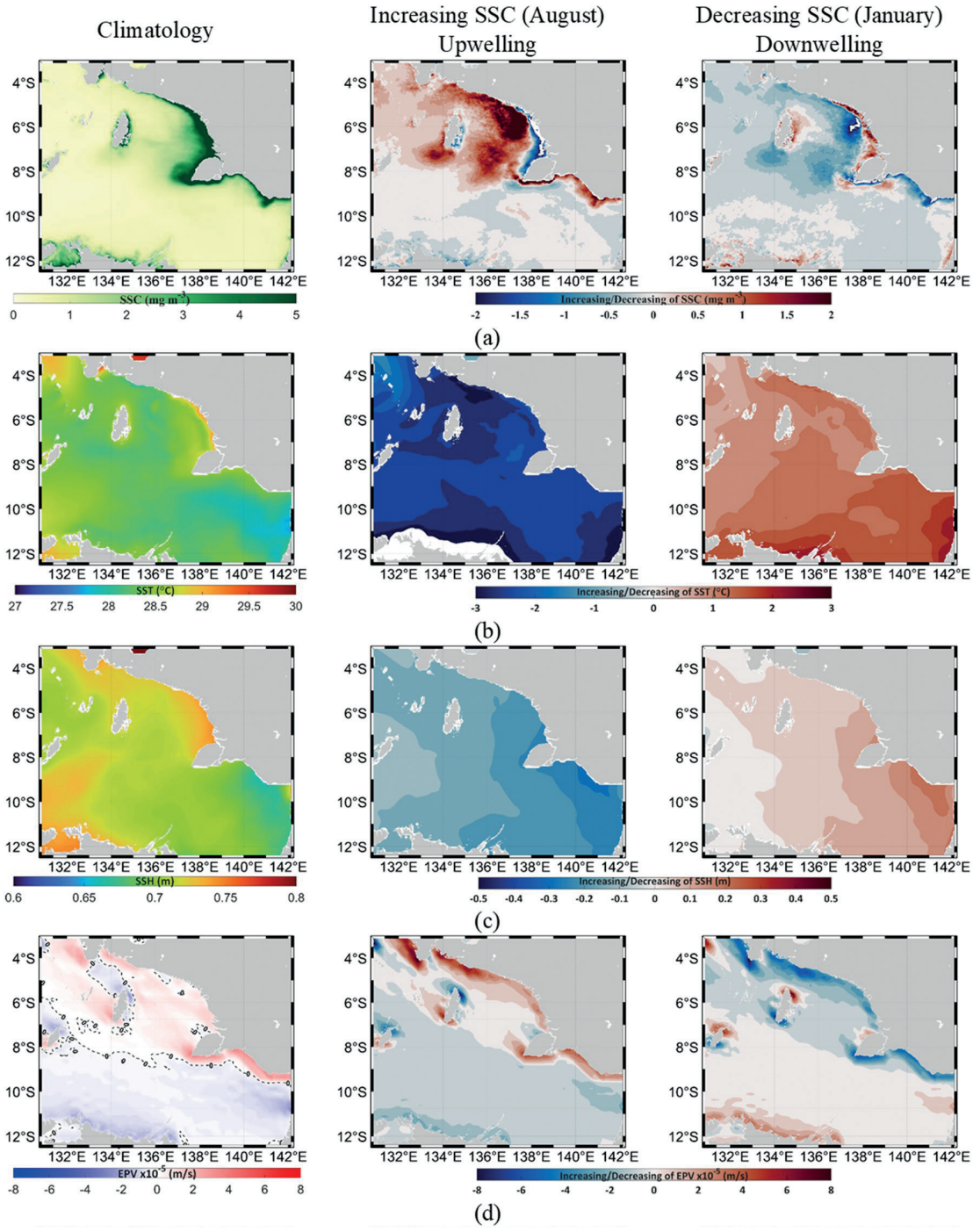

Fig. 11 - Spatial distributions of climatological mean conditions and long-term increasing and decreasing trends of SSC (a) during 1998–2022. The environmental parameters used to characterise these patterns include SST (b), significant wave height (c), EPV (d), SSS (e), SSD (f), total precipitation (g), and river discharge (h).

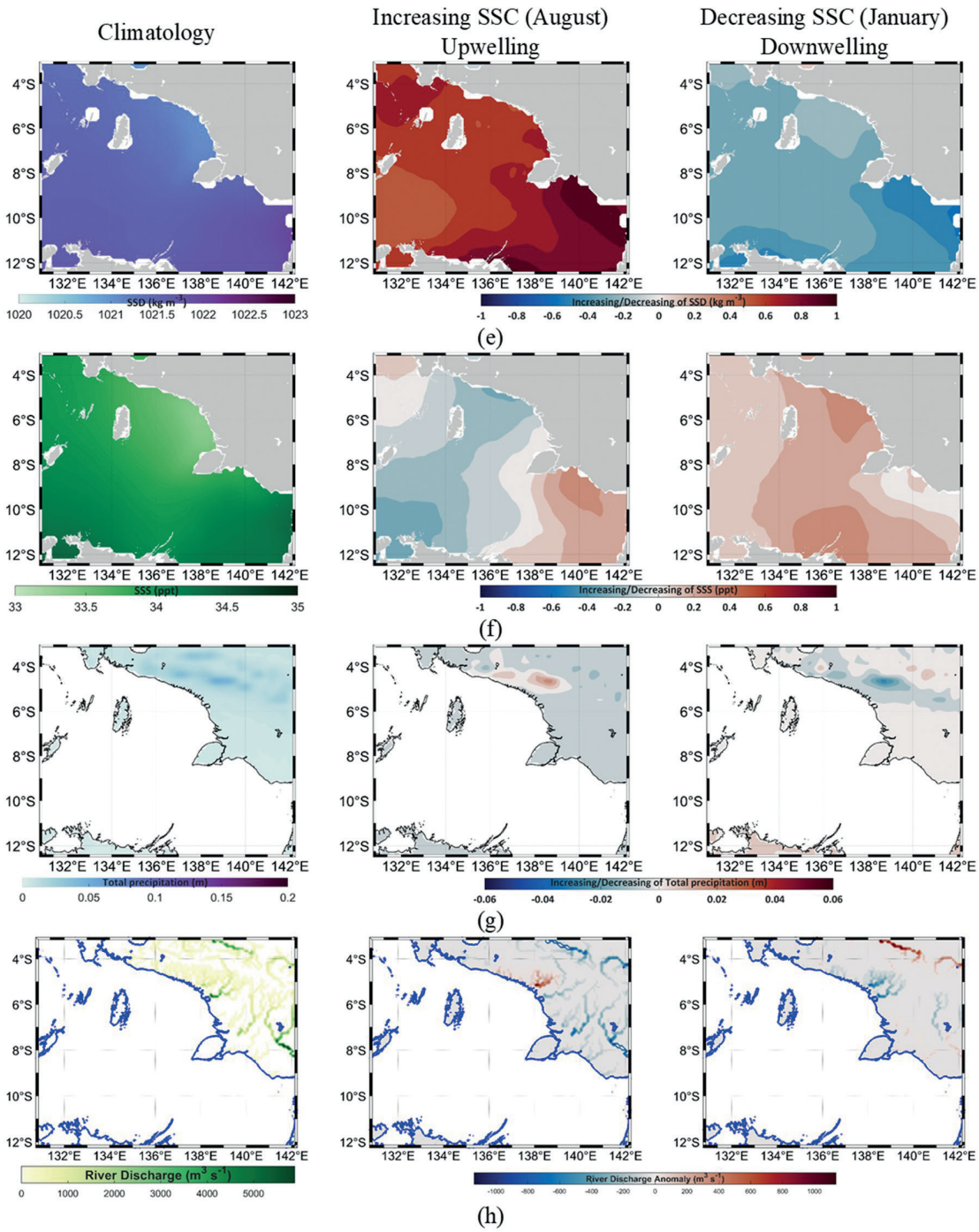

Fig. 11 - continued.

upwelling. Although river discharge persists year-round, it decreases substantially during this dry-season month, producing a negative anomaly across most major river systems in southern Papua. Thus, while riverine influence remains present, it is at its annual minimum. Conversely, a decline in SSC near northern Australia and Trangan Island indicates the strengthening of downwelling

in those areas. Evidence for upwelling is further supported by widespread decreases in SST and SSH, particularly in south-eastern Arafura, where sharply reduced SSH signals enhanced Ekman pumping. In addition, the expansion of low-salinity waters near the northern Australian and Papuan coasts primarily reflects freshwater input from river plumes and precipitation, while concurrent upwelling enhances nutrient supply through the upward transport of more saline subsurface waters.

Monsoon-driven variability in EPV further reinforces this interpretation. The simultaneous increase and decrease of EPV across different islands reflect the intensification of monsoon winds during this period. Likewise, enhanced precipitation over Papua coincides with elevated offshore SSC, emphasising the role of rainfall-mediated nutrient delivery in sustaining phytoplankton blooms. Collectively, these patterns suggest that during peak monsoon conditions, both horizontal advection and vertical pumping are strongly modulated by wind forcing and freshwater input, jointly shaping the growth environment for phytoplankton.

By contrast, during the peak of the NW monsoon in January, the cessation of upwelling along the Papua coast coincides with intensified downwelling, effectively reversing the SSC gradient observed during the SE monsoon. The increase in SSC along island coasts, combined with a decline offshore, highlights the interaction between downwelling and river discharge. Rising SST near the coast provides further evidence for downwelling, while negative EPV values point to enhanced stratification that inhibits the upward flux of cold, nutrient-rich water, thereby limiting offshore productivity. Freshwater inputs from river discharge and precipitation also reduce SSS and SSD, further modulating SSC. These inputs are particularly pronounced during January, when discharge from major southern Papuan rivers exceeds ~3000 m^3/s, representing a strong positive anomaly. This massive seasonal surge of freshwater, nutrients, and sediments directly sustains the observed coastal SSC increase.

Fig. 11 illustrates these processes, showing spatial variations in river discharge, SST, SSH, EPV, SSS, SSD, and precipitation that highlight the physical controls on SSC variability. The observed increase in SSH during the NW monsoon corresponds to the dominance of northwesterly winds, which promote Ekman convergence and downwelling, further modulated by regional bathymetry and the narrowing of cross-sectional passages. Distinct climatological SSD patterns between the Torres Strait and the north-western Papua coast likely reflect differences in EPV intensity, further underscoring the complexity of physical–biological interactions in the Arafura Sea. Overall, these climatological analyses confirm that variability in SSC is governed by temporally dynamic and spatially heterogeneous forcing mechanisms and that integrated observational frameworks are essential for capturing the full ecosystem response.

3.5. Interannual variability of sea surface chlorophyll-a, sea surface temperature, and total precipitation revealed by the empirical orthogonal function

The *EOF* analysis of deseasonalised SSC reveals that the four highest *EOF* modes collectively explain 64% of the total variance (Fig. 12). The first mode (*EOF*1) accounts for the highest variability, primarily concentrated around the southern coast of Papua. The correlation between the *PC*s (*PC*1–*PC*4) and the ONI is 3.81%, 23.05%, 10.73%, and 11.02%, respectively. These results indicate a weak correlation between SSC variability and ENSO, suggesting that other factors play a more dominant role in interannual SSC fluctuations.

*EOF*1 highlights multiple peaks of high SSC anomalies occurring in September 2008, September 2009, and November 2015, with an amplification of 0.55–0.59 $mg \cdot m^{-3}$. The recurrence of high SSC anomalies during late dry season months coincides with the peak of south-easterly winds,

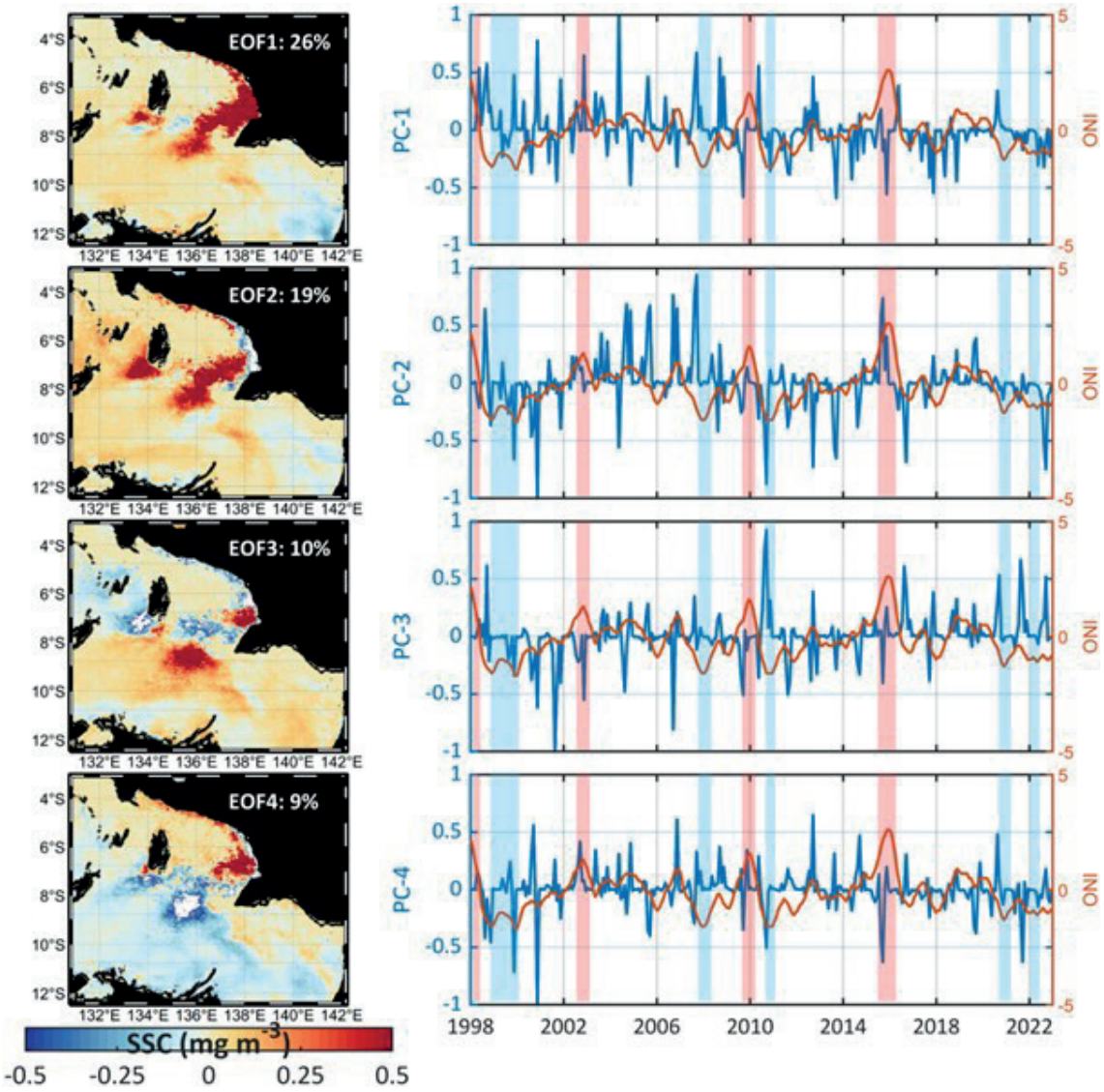

Fig. 12 - Deseasonalised interannual variability of SSC explained by the four highest *EOF* modes (accounting for 63% of the total variability) in spatial (left) and temporal (right) terms from 1998 to 2022. Red and blue transparent boxes consecutively highlight the ONI value, which broke the ±1 threshold, indicating an extreme period of the ENSO phenomenon.

reinforcing the interpretation that monsoon-driven vertical nutrient flux is the primary driver of interannual SSC enhancement. The first three *EOF* modes suggest that high SSC anomalies predominantly occur offshore, indicating a strong influence of coastal upwelling and nutrient runoff. Meanwhile, the consistent high variability of SSC near the coast across multiple modes underscores the continuous role of river discharge in modulating SSC concentrations. These spatial patterns suggest a dual-source nutrient regime, with offshore anomalies linked to physical oceanographic forcing and nearshore anomalies reflecting sustained fluvial input.

The *EOF* analysis of deseasonalised SST indicates that the *EOF*1 captures 82% of the total variability, highlighting its dominant role in governing SST fluctuations in the Arafura Sea (Fig.

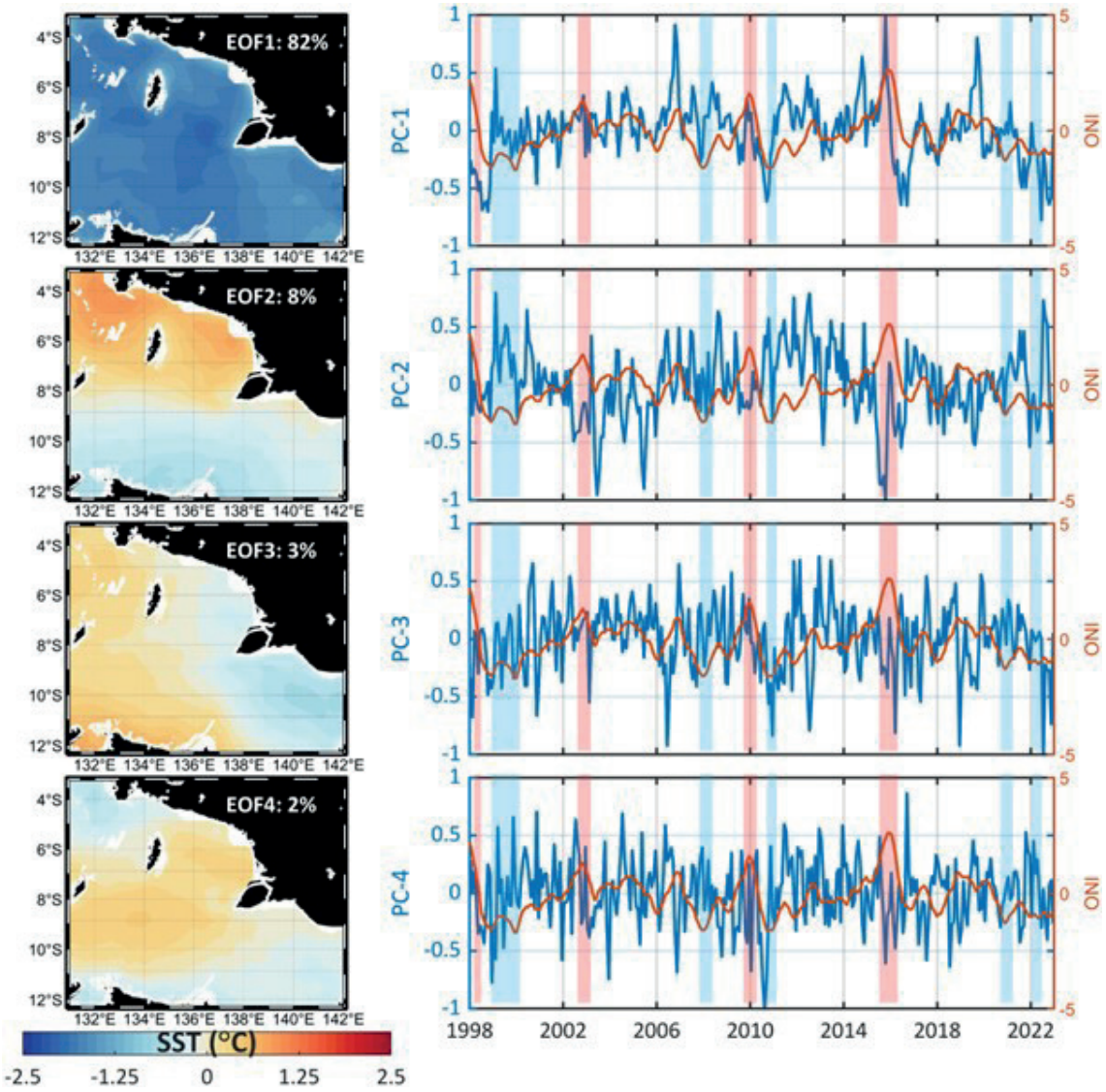

Fig. 13 - Deseasonalised interannual variability of SST explained by the four highest *EOF* modes (accounting for 95% of the total variability) in spatial (left) and temporal (right) terms from 1998 to 2022. Red and blue transparent boxes highlight the ONI value, which broke the ±1 threshold, indicating an extreme period of the ENSO phenomenon.

13). *EOF*1 shows that most SST intensifications occur during periods of moderate ONI values, suggesting that SST variability is not solely driven by extreme ENSO events but rather by a combination of regional ocean–atmosphere interactions.

Periods of prolonged negative SST anomalies are observed from February 1998 to October 2000, corresponding to a significant cooling event. However, in November 2015, *PC*1 and the ONI exhibited an inverse relationship, which may be attributed to a time lag in the propagation of warm western Pacific water masses through the Indonesian Throughflow (ITF) pathways. This lag effect is further supported by the delayed decrease in *PC*1 following the event. Such lagged responses point to the influence of remote ocean circulation and thermal inertia, which may decouple SST behaviour from real-time ENSO indices.

Spatially, *EOF*2 exhibits a N-S SST contrast, while *EOF*3 reveals W-E SST differences, and *EOF*4

highlights positive SST anomalies concentrated in the central Arafura Sea. Notably, regions exhibiting high SST variability often coincide with areas of high SSC variability, particularly in the mid-Arafura Sea. This co-occurrence suggests that SST fluctuations may influence phytoplankton dynamics through their impact on vertical mixing and stratification. Thus, SST not only serves as a passive indicator but also acts as a modulator of nutrient availability through its role in water column structure.

The *EOF* analysis of total precipitation reveals that the first four modes explain 82% of the total variance (Fig. 14). *EOF*1 primarily captures negative precipitation anomalies along the Papua coast, contrasting with positive anomalies over inland Papua. This pattern suggests that coastal

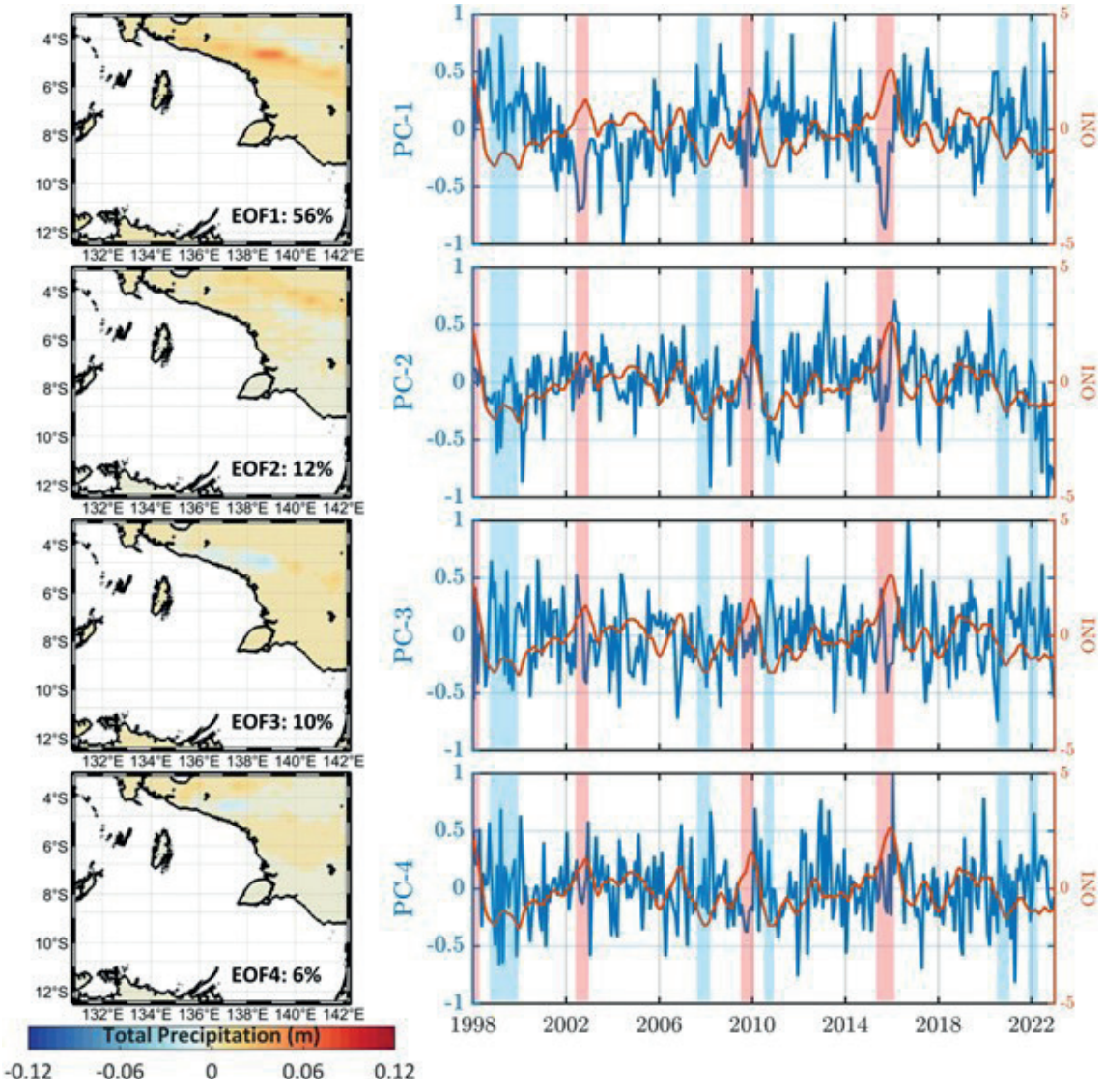

Fig. 14 - Deseasonalised interannual variability of total precipitation explained by the four highest EOF modes (accounting for 82% of the total variability) in spatial (left) and temporal (right) terms from 1998 to 2022. Red and blue transparent boxes consecutively highlight the ONI value, which broke the ±1 threshold, indicating an extreme period of the ENSO phenomenon.

upwelling and river discharge exert a stronger influence on SSC than dilution effects associated with precipitation. The spatial decoupling between inland and coastal rainfall emphasises the limited role of direct precipitation in phytoplankton bloom formation, compared to fluvial nutrient transport.

The spatial distribution of the remaining three *EOF* modes highlights more localised precipitation anomalies near the coast. Specifically, *EOF*2 exhibits scattered negative anomalies in the south, *EOF*3 presents a relatively uniform pattern with distinct anomalies in north-western Papua, and *EOF*4 displays a more diffuse precipitation pattern. These modes suggest that interannual precipitation variability is spatially heterogeneous, which may influence the timing and magnitude of nutrient delivery to coastal waters.

The corresponding *PC* time series (*PC*1–*PC*4) shows weak correlations with the ONI, with -values of 0.368, 0.363, 0.195, and 0.099, respectively. Additionally, during extreme ENSO events, the *PC*s exhibit contrasting precipitation patterns, further indicating that the ENSO is not the sole driver of interannual precipitation variability.

Changes in water mass transport through the ITF pathways under a changing climate may also contribute to the observed precipitation patterns. Previous studies have found that ENSO-affected regions experience 33–50% higher rainfall variability compared to non-ENSO-affected areas (Nicholls, 1988), highlighting the complex interplay between meteorological and oceanographic factors in modulating precipitation in the Arafura Sea.

4. Discussion

The Copernicus Marine products utilised in this study have undergone rigorous qualification and validation through continuous scientific assessments, ensuring their reliability and appropriateness for regional-scale oceanographic investigations (von Schuckmann *et al.*, 2016; Le Traon *et al.*, 2019). However, satellite-derived SSC estimates may exhibit positive biases in coastal waters due to the optical influence of high suspended sediment loads and coloured dissolved organic matter originating from riverine inputs (Napitupulu *et al.*, 2023; Quan and Chen, 2023). Such effects should be carefully considered when interpreting SSC variability, particularly within nearshore environments influenced by fluvial plumes and turbid water masses.

This study investigates the mechanisms driving SSC enhancement in the Arafura Sea, a region of ecological and economic significance. Phytoplankton, as the foundation of marine ecosystems, play a crucial role in primary production, with SSC serving as a key proxy for their abundance (Batteen *et al.*, 1995; Huang, 1996). Understanding the spatiotemporal variability of SSC is essential for assessing ocean health, fishery productivity, and regional climate interactions (Bingham and Brodnitz, 2021; Chilukoti *et al.*, 2024; Maier *et al.*, 2025). The Arafura Sea is influenced by complex oceanographic processes, including monsoonal winds, river discharge, and the ENSO. We hypothesised that SSC enhancement is primarily driven by river discharge, precipitation, and seasonal monsoon dynamics, with potential modulation by the ENSO. Using 24 years (1998–2022) of oceanographic data (SST, SSS, SSD, EPV, total precipitation, and river discharge), we analysed the interplay among these factors. Our findings confirm this hypothesis and highlight the Arafura Sea as a dynamic interface where atmosphere, ocean, and land interactions jointly regulate productivity, differing from neighbouring tropical seas where the ENSO exerts greater control.

4.1. Seasonal variability of sea surface chlorophyll-a and its forcing mechanisms

Our results revealed distinct seasonal SSC patterns, with maximum concentrations occurring in July during the SE monsoon, coinciding with intensified upwelling, as indicated by positive EPV and reduced SSH. Conversely, the lowest SSC was observed in December, aligning with the NW monsoon and prevailing downwelling conditions. These seasonal variations are consistent with monsoon-driven Ekman dynamics, reinforcing previous findings on upwelling in the region. This seasonal oscillation forms the backbone of phytoplankton seasonality in the Arafura Sea, with upwelling acting as a physical trigger and riverine input sustaining nearshore productivity.

The relatively stable SSC levels along the southern Papua coastline suggest a continuous supply of nutrients, primarily from river discharge and terrestrial inputs, which may be further modulated by precipitation and anthropogenic activities (Geng *et al.*, 2021). Offshore SSC enhancement, however, indicates an interplay between mesoscale eddies and river plumes, emphasising the complexity of physical and biogeochemical interactions (Chenillat *et al.*, 2024). While mesoscale eddies facilitate vertical nutrient mixing, river discharge supplies organic and inorganic nutrients offshore, creating hotspots of phytoplankton growth (Cordier *et al.*, 2025). Such interactions imply that productivity hotspots may form through the coupling of localised wind-driven upwelling and nutrient transport pathways, not solely from basin-scale processes.

EPV analysis revealed that peak upwelling occurs in July, while downwelling dominates in February, consistent with seasonal wind forcing. Upwelling intensity is strongest along the southern Papua coast in September, while the northern Papua coast experiences downwelling during the NW monsoon. The role of island orientation and wind stress is evident, influencing localised Ekman transport and modulating SSC distribution. SSH analysis corroborates these upwelling patterns, with minimum SSH (0.58 m) in July and maximum SSH (0.81 m) in December, reflecting the seasonal alternation between upwelling and downwelling regimes. Together, EPV and SSH provide robust physical indicators that closely align with SSC seasonality, validating their use as proxies for productivity shifts in monsoon-influenced systems.

SST exhibited an inverse relationship with upwelling, with minimum temperatures (25.95 °C) in August during peak upwelling and maximum temperatures (30.05 °C) in December during peak downwelling. This confirms SST as a robust upwelling indicator, consistent with previous studies (Arcos and Wilson, 1984; Napitupulu *et al.*, 2025b). Meanwhile, precipitation showed a relatively uniform seasonal distribution, with maximum rainfall (0.0142 m) in March and minimum rainfall (0.0083 m) in July, suggesting a secondary but notable influence on SSC dynamics through nutrient runoff and water column stratification. Although precipitation alone does not dictate SSC concentrations, its interaction with river discharge significantly modulates coastal nutrient loading and mixing conditions.

4.2. Regional and interannual variability of sea surface chlorophyll-a

Regional correlation analysis revealed strong spatial variability in the relationship between SSC and EPV. In Region A, SSC and EPV exhibit a moderate negative correlation (-0.59), likely due to the coastal orientation effect, which influences wind-driven upwelling patterns. In contrast, Region B and Region C exhibit strong positive correlations (0.78 and 0.85, respectively), indicating upwelling-driven phytoplankton blooms. Additionally, SSC in Region B correlates positively with precipitation (0.8), highlighting the role of nutrient runoff in phytoplankton growth. Such spatial heterogeneity highlights the importance of considering coastline orientation and bathymetric complexity when predicting regional upwelling intensity, as small-scale wind-topography

interactions can create productivity hotspots or downwelling shadows (He and Mahadevan, 2021). These spatial differences emphasise the importance of geomorphological and atmospheric coupling in regulating nutrient delivery mechanisms across subregions.

EOF analyses highlight that SSC variability is most pronounced along the Papua coast, reflecting the sustained influence of river discharge (Börger *et al.*, 2024). The weak correlations between SSC, SST, and precipitation with the ONI suggest that interannual variability is primarily controlled by regional processes rather than ENSO forcing (Kealoha *et al.*, 2020; Rashid *et al.*, 2020; Wang *et al.*, 2022). Notably, SST fluctuations in regions of high SSC variability, particularly in the mid-Arafura Sea, likely regulate phytoplankton blooms through their impact on vertical mixing and stratification (Liu *et al.*, 2019). Meanwhile, precipitation, though not a dominant driver, modulates nutrient input and water column stability via riverine discharge, thereby shaping phytoplankton distribution (Xu *et al.*, 2021, 2024).

Our findings underscore the dominant role of monsoon-driven upwelling and river discharge in shaping SSC variability in the Arafura Sea. While the ENSO and precipitation exert secondary influences, the seasonal monsoon cycle and terrestrial nutrient input remain the key drivers of phytoplankton blooms. During the SE monsoon, SSC increases due to strong upwelling, as evidenced by enhanced EPV, reduced SST, and lower SSH. The interaction of Ekman-driven upwelling and river discharge facilitates phytoplankton growth, leading to distinct offshore SSC anomalies. In contrast, the NW monsoon is dominated by downwelling, with higher SST, increased SSH, and lower SSC, illustrating the seasonal reversal of oceanographic conditions (Kämpf, 2015; Naik *et al.*, 2020).

The *EOF* results further highlight the limited direct influence of the ENSO on SSC variability. Although the ENSO affects regional atmospheric circulation and ITF transport, its impact on SSC is relatively weak compared to seasonal monsoonal forcing and local hydrodynamic processes (Racault *et al.*, 2017; Koropitan *et al.*, 2021). This suggests that local ocean–atmosphere interactions and terrestrial nutrient inputs are the primary regulators of phytoplankton dynamics in the Arafura Sea (Dewi *et al.*, 2018). This decoupling from the ENSO makes the Arafura Sea a unique tropical system where internal regional dynamics override broader climatic oscillations, underscoring the need for localised environmental monitoring frameworks.

5. Conclusions

This study analyses the significance of various oceanographic features on SSC dynamics in the Arafura Sea using seasonal and interannual analyses. The SSC analysis results indicate that the relatively steady level of SSC along the coast of the surrounding island is seasonally and interannually variable, due to continuous river discharge. On the other hand, the SSC offshore dynamics show a prominent role of the monsoon season modulating the region, which subsequently affects the EPV dynamics and rainfall precipitation. The high total precipitation during the SE monsoon gives constructive enhancement for the abundance of SSC, besides the role of coastal upwelling and river discharge. The strengthening EPV throughout the climatological period reflects an intensifying monsoon wind. On the other hand, the NW monsoon indicates the role of continuous river discharge along the coast of the surrounding island, demonstrated by a prominent SSC gradient in the region. Moreover, the interannual analysis reveals that SSC dynamics are not solely modulated by the ENSO phenomenon, indicating the influence of other atmospheric and oceanic processes. Moreover, the SST dynamics indicate inverse correlation with the ONI, revealing a time lag associated with the western Pacific water mass transport.

The interannual dynamics of total precipitation indicate a high variability near the middle and north-western Papua, indicating the dominant role of nutrient runoff around the region. These findings provide new insight into the dual forcing mechanisms, monsoonal upwelling and terrestrial runoff, that govern phytoplankton variability in marginal tropical seas like the Arafura. By integrating long-term satellite data with regional *EOF* analysis, this study confirms that local ocean-atmosphere-land interactions outweigh large-scale climate modes, such as the ENSO, in regulating SSC variability. Such knowledge is essential for enhancing the accuracy of ecosystem forecasting, particularly for predicting seasonal productivity that supports key fisheries in the region.

Acknowledgments. The authors sincerely thank the editor and anonymous reviewers for their valuable suggestions and constructive comments, which greatly improved the quality of this manuscript. The authors also acknowledge the use of MATLAB software for generating all figures and the assistance of artificial intelligence tools for language refinement.

REFERENCES

Ahkam M.F. and Tarya A.; 2023: *Estimation of the potential of large pelagic fish fisheries using satellite data in the Banda and Arafura Seas.* Devotion J. Res. Community Serv., 4, 2338-2352, doi: 10.59188/DEVOTION.V4I12.646.

Arcos D.F. and Wilson R.E.; 1984: *Upwelling and the distribution of chlorophyll-a within the bay of Concepción, Chile.* Estuarine Coastal Shelf Sci., 18, 25-35, doi: 10.1016/0272-7714(84)90004-0.

Auricht H., Mosley L., Lewis M. and Clarke K.; 2022: *Mapping the long-term influence of river discharge on coastal ocean chlorophyll*-a. Remote Sens. Ecol. Conserv., 8, 629-643, doi: 10.1002/rse2.266.

Babagolimatikolaei J.; 2024: *Effects of variations in Po River discharge on physical water characteristics and chlorophyll-a levels in the Gulf of Manfredonia.* Geosci. Lett., 11, 1-19, doi: 10.1186/S40562-024-00342-W/FIGURES/13.

Basu S. and Mackey K.R.M.; 2018: *Phytoplankton as key mediators of the biological carbon pump: their responses to a changing climate.* Sustainability, 10, 869, doi: 10.3390/su10030869.

Batteen M.L., Collins C.A., Gunderson C.R. and Nelson C.S.; 1995: *The effect of salinity on density in the California current system.* J. Geophys. Res.: Oceans, 100, 8733-8749, doi: 10.1029/95JC00424.

Bingham F.M. and Brodnitz S.; 2021: *Sea surface salinity short-term variability in the tropics*. Ocean Sci., 17, 1437-1447, doi: 10.5194/os-17-1437-2021.

Börger L., Schindelegger M., Zhao M., Ponte R.M., Löcher A., Uebbing B. and Penduff T.; 2024: *Chaotic oceanic excitation of low-frequency polar motion variability.* Earth Syst. Dyn., 16, 75-90, doi: 10.5194/esd-16-75-2025.

Bravo L., Ramos M., Astudillo O., Dewitte B. and Goubanova K.; 2016: *Seasonal variability of the Ekman transport and pumping in the upwelling system off central-northern Chile based on a high-resolution atmospheric regional model (WRF)*. Ocean Sci., 12, 1049-1065, doi: 10.5194/OS-12-1049-2016.

Brewin R.J., Morán X.A.G., Raitsos D.E., Gittings J.A., Calleja M.L., Viegas M. and Hoteit I.; 2019: *Factors regulating the relationship between total and size-fractionated chlorophyll-a in coastal waters of the Red Sea.* Front. Microbiol., 10, 1964, doi: 10.3389/fmicb.2019.01964.

Buton I., Tubalawony S., Wattimena A.A., Jurusan M.C., Kelautan I. and Perikanan F.; 2023: *Variabilitas hidrometeorologi permukaan laut arafura pada saat fenomena ENSO.* J. Laut Pulau: Hasil Penelitian Kelautan, 2, 32-50, doi: 10.30598/JLPVOL2ISS2PP32-50 (in Indonesian).

Chenillat F., Deshaies E., Arens A. and Penven P.; 2024: *Role of mesoscale eddies in the biogeochemistry of the Mozambique Channel.* Front. Mar. Sci., 11, 1402776, doi: 10.3389/fmars.2024.1402776.

Chilukoti N., Nimmakanti M. and Chowdary J.S.; 2024: *Recent two decades witness an uptick in monsoon depressions over the northern Arabian Sea.* npj Clim. Atmos. Sci., 7, 183, doi: 10.1038/s41612-024-00727-w.

Cordier A., Bendtsen J., Daugbjerg N., From N., Jónasdóttir S.H., Mousing E.A. and Richardson K.; 2025: *Patchiness of plankton ecosystem structure due to nutrient mixing along the shelf edge in the North Sea*. Sci. Rep., 15, 1183, doi: 10.1038/s41598-024-83811-8.

Correa-Ramirez M.A., Hormazábal S. and Yuras G.; 2007: *Mesoscale eddies and high chlorophyll concentrations off central Chile (29°-39°S)*. Geophys. Res. Lett., 34, 12604, doi: 10.1029/2007GL029541.

Dewi D.M.P.R., Fatmasari D., Kurniawan A. and Munandar M.A.; 2018: *The impact of ENSO on regional chlorophyll-a anomaly in the Arafura Sea*. IOP Conf. Ser., Earth Environ. Sci., 139, 012020, doi: 10.1088/1755-1315/139/1/012020.

Fathurohman A., Napitupulu G., Fujiawati G. and Napitupulu M.; 2025: *Impact of significant wave height, wind speed, and precipitation variability on shipping safety in Indonesian Archipelagic Sea lanes*. Bull. Mar. Geol., 40, 44-61, doi: 10.32693/bomg.40.1.2025.895.

Fernández-González C., Tarran G.A., Schuback N., Woodward E.M.S., Arístegui J. and Marañón E.; 2022: *Phytoplankton responses to changing temperature and nutrient availability are consistent across the tropical and subtropical Atlantic*. Commun. Biol., 5, 1035, doi: 10.1038/s42003-022-03971-z.

Gao J., Wang J. and Wang F.; 2019: *Response of near-inertial shear to wind stress curl and sea level*. Sci. Rep., 9, 20417, doi: 10.1038/s41598-019-56822-z.

Geng B., Xiu P., Liu N., He X. and Chai F.; 2021: *Biological response to the interaction of a mesoscale eddy and the river plume in the northern South China Sea.* J. Geophys. Res. Oceans, 126, e2021JC017244, doi: 10.1029/2021JC017244.

Gomez-Gesteira M., Moreira C., Alvarez I. and de Castro M.; 2006: *Ekman transport along the Galician coast (northwest Spain) calculated from forecasted winds.* J. Geophys. Res. Oceans, 111, doi: 10.1029/2005JC003331.

Gui J. and Sun J.; 2024: *Phytoplankton carbon to chlorophyll-a model development: a review.* Front. Mar. Sci., 11, 1466072, doi: 10.3389/fmars.2024.1466072.

Gustiantini L., Piranti S.A., Zuraida R., Hyun S., Ranawijaya D.A.S. and Prabowo F.X.H.H.; 2018: *Foraminiferal analysis related to paleoceanographic changes of Arafura Sea and surrounding during Holocene.* Bull. Mar. Geol., 33, 105-118, doi: 10.32693/BOMG.33.2.2018.571.

He J. and Mahadevan A.; 2021: *How the source depth of coastal upwelling relates to stratification and wind.* J. Geophys. Res. Oceans, 126, e2021JC017621, doi: 10.1029/2021JC017621.

He T., Li J., Xie L. and Zheng Q.; 2024: *Response of chlorophyll-a to rainfall event in the basin of the South China Sea: statistical analysis.* Mar. Environ. Res., 199, 106576, doi: 10.1016/J.MARENVRES.2024.106576.

Hidaka K.; 1972: *Physical oceanography of upwelling.* Geoforum, 3, 9-21, doi: 10.1016/0016-7185(72)90082-6.

Huang M.-J.; 1996: *The effect of salinity on density in the Leeuwin current system*. Master's Thesis in Science in Physical Oceanography, Naval Postgraduate School, Monterey, CA, USA, 76 pp.

Huang W., Mukherjee D. and Chen S.; 2011: *Assessment of Hurricane Ivan impact on chlorophyll-a in Pensacola Bay by MODIS 250 m remote sensing.* Mar. Pollut. Bull., 62, 490-498, doi: 10.1016/J.MARPOLBUL.2010.12.010.

Hughes P. and Barton E.D.; 1974: *Stratification and water mass structure in the upwelling area off northwest Africa in April/May 1969.* Deep Sea Res. Oceanogr. Abstr., 21, 611-628, doi: 10.1016/0011-7471(74)90046-1.

Huisman J., Pham Thi N.N., Karl D.M. and Sommeijer B.; 2006: *Reduced mixing generates oscillations and chaos in the oceanic deep chlorophyll maximum.* Nature, 439, 322-325, doi: 10.1038/nature04245.

Huot Y., Babin M., Bruyant F., Grob C., Twardowski M.S. and Claustre H.; 2007: *Relationship between photosynthetic parameters and different proxies of phytoplankton biomass in the subtropical ocean.* Biogeosci., 4, 853-868, doi: 10.5194/bg-4-853-2007.

Ilahude A.G., Hortle K. and Kusmanto E.; 2004: *Oceanography of coastal and riverine waters around Timika, west central Irian Jaya, Arafura Sea.* Cont. Shelf Res., 24, 2511-2520, doi: 10.1016/j.csr.2004.07.020.

Kämpf J.; 2015: *Undercurrent-driven upwelling in the northwestern Arafura Sea.* Geophys. Res. Lett., 42, 9362-9368, doi: 10.1002/2015GL066163.

Kämpf J.; 2016: *On the majestic seasonal upwelling system of the Arafura Sea.* J. Geophys. Res. Oceans, 121, 1218-1228, doi: 10.1002/2015JC011197.

Karima S., Ningsih N.S., Tisiana A.R. and Napitupulu G.; 2025: *Water mass vertical mixing in the Sulawesi Sea and Makassar Strait during the second transition monsoon.* Earth Planet. Sci., 4, 73-88, doi: 10.36956/eps.v4i1.2061.

Kealoha A.K., Shamberger K.E., DiMarco S.F., Thyng K.M., Hetland R.D., Manzello D.P. and Enochs I.C.; 2020: *Surface water CO2 variability in the Gulf of Mexico (1996-2017)*. Sci. Rep., 10, 12279, doi: 10.1038/s41598-020-68924-0.

Khadami F., Suprijo T., Hidayat A.R., Radjawane I.M., Tarya A. and Napitupulu G.; 2025: *Near-bed flow dynamics and bed shear stress in a mangrove-vegetated estuary.* IOP Conf. Ser., Earth Environ. Sci., 1464, 012014, doi: 10.1088/1755-1315/1464/1/012014.

Koropitan A.F. and Osawa T.; 2021: *Modeling small-pelagic fish biomass in the Indonesian seas: climate variability and climate change impacts.* IOP Conf. Ser., Earth Environ. Sci., 944, 012069, doi: 10.1088/1755-1315/944/1/012069.

Kubryakova E.A., Kubryakov A.A. and Stanichny S.V.; 2018: *Impact of winter cooling on water vertical entrainment and intensity of phytoplankton bloom in the Black Sea.* Phys. Oceanogr., 25, 191-206, doi: 10.22449/1573-160X-2018-3-191-206.

Le Traon P.Y., Reppucci A., Alvarez Fanjul E., Aouf L., Behrens A., Belmonte M., Bentamy A., Bertino L., Brando V.E., Brandt Kreiner M., Benkiran M., Carval T., Ciliberti S.A., Claustre H., Clementi E., Coppini G., Cossarini G., De Alfonso-Muñoyerro M., Delamarche A., Dibarboure G., Dinessen F., Drevillon M., Drillet Y., Faugere Y., Fernández V., Fleming A., Garcia-Hermosa M.I., García Sotillo M., Garric G., Gasparin F., Giordan C., Gehlen M., Gregoire M.L., Guinehut S., Hamon M., Harris C., Hernandez F., Hinkler J.B., Hoyer J., Karvonen J., Kay S., King R., Lavergne T., Lemieux-Dudon B., Lima L., Mao C., Martin M.J., Masina S., Melet A., Nardelli B.B., Nolan G., Pascual A., Pistoia J., Palazov A., Piolle J.F., Pujol M.I., Pequignet A.C., Peneva E., Pérez Gómez B., Petit de la Villeon L., Pinardi N., Pisano A., Pouliquen S., Reid R., Remy E., Santoleri R., Siddorn J., She J., Staneva J., Stoffelen A., Tonani M., Vandenbulcke L., von Schuckmann K., Volpe G., Wettre C. and Zacharioudaki A.; 2019: *From observation to information and users: the Copernicus Marine Service perspective.* Front. Mar. Sci., 6, 234, doi: 10.3389/fmars.2019.00234.

Liu C., Sun Q., Xing Q., Wang S., Tang D., Zhu D. and Xing X.; 2019: *Variability in phytoplankton biomass and effects of sea surface temperature based on satellite data from the Yellow Sea, China.* Plos one, 14, e0220058, doi: 10.1371/journal.pone.0220058.

Lukman A.A., Tarya A. and Pranowo W.S.; 2024: *Spatial and temporal pattern of thermal front in Republic of Indonesia fisheries management area 571 (FMA 571).* IOP Conf. Ser., Earth Environ. Sci., 1350, 012033, doi: 10.1088/1755-1315/1350/1/012033.

Maier J., Burdanowitz N., Schmiedl G. and Gaye B.; 2025: *Spatial and temporal variability in sea surface temperatures and monsoon dynamics in the northwestern Arabian Sea during the last 43 kyr*. Clim. Past, 21, 279-297, doi: 10.5194/cp-21-279-2025.

McCain C.R., Hooker S., Feldman G. and Bontempi P.; 2006: *Satellite data for ocean biology, biogeochemistry and climate research.* Eos, Trans. Am. Geophys. Union, 87, 337-343, doi: 10.1029/2006EO340002.

Meng P.J., Tew K.S., Hsieh H.Y. and Chen C.C.; 2017: *Relationship between magnitude of phytoplankton blooms and rainfall in a hyper-eutrophic lagoon: a continuous monitoring approach.* Mar. Pollut. Bull., 124, 897-902, doi: 10.1016/J.MARPOLBUL.2016.12.040.

Meyssignac B., Piecuch C.G., Merchant C.J. and Racault M.-F., Palanisamy H., MacIntosh C., Sathyendranath S. and Brewin R.; 2017: *Causes of the regional variability in observed sea level, sea surface temperature and ocean colour over the period 1993-2011.* Surv. Geophys., 38, 187-215, doi: 10.1007/s10712-016-9383-1.

Nagi A., Jamaluddin J., Napitupulu G., Nurdjaman S., Setyobudiandi I. and Radjawane I.M.; 2023: *Pengelolaan dan Pemanfaatan Kawasan Pesisir Pulau Miangas Sebagai Pulau Kecil Terluar Indonesia.* J. Kebijakan Perikanan Indonesia, 15, 33-48, doi: 10.15578/jkpi.15.1.2023.%25p (in Indonesian).

Naik S., Mishra R.K., Sahu K.C., Lotliker A.A., Panda U.S. and Mishra P.; 2020: *Monsoonal influence and variability of water quality, phytoplankton biomass in the tropical coastal waters - A multivariate statistical approach.* Front. Mar. Sci., 7, 648, doi: 10.3389/fmars.2020.00648.

Napitupulu G.; 2025a: *Spatiotemporal variability of coastal upwelling in response to monsoonal forcing and semi-enclosed basins in the Indonesian and adjacent seas.* Ocean Dyn., 75, 1-20, doi: 10.1007/s10236-025-01706-2.

Napitupulu G.; 2025b: *Influence of mesoscale eddies on marine cold spells and heatwaves in Arafura Sea.* Mar. Syst. Ocean Technol., 20, 1-14, doi: 10.1007/s40868-025-00189-6.

Napitupulu G.; 2025c: *Eddy-induced modulation of marine heatwaves and cold spells in a tropical region: a case study in the Natuna sea area.* Ocean Dyn., 75, 28, doi: 10.1007/s10236-025-01673-8.

Napitupulu G., Nuruddin M.F., Fekranie N.A. and Magdalena I.; 2021: *Analysis of wind generated wave characteristics by SWAN model in Balikpapan Bay.* IOP Conf. Ser., Earth Environ. Sci., 930, 012067, doi: 10.1088/1755-1315/930/1/012067.

Napitupulu G., Nurdjaman S., Fekranie N.A., Suprijo T. and Subehi L.; 2022: *Analysis of upwelling in the southern Makassar Strait in 2015 using Aqua-MODIS satellite image.* J. Water Res. Ocean Sci., 11, 64-70*,* doi: 10.11648/J.WROS.20221104.11.

Napitupulu G., Fekranie N.A., Nurdjaman S., Suprijo T. and Subehi L.; 2023: *Analysis of upwelling variations caused by ENSO intensification in the southern Makassar Strait.* In: Proc. International Conference on Radioscience, Equatorial Atmospheric Science and Environment and Humanosphere Science, INCREASE 2023, Singapore, Indonesia, Springer Series in Geomechanics and in Geoengineering, vol. 290, pp. 437-448, doi:10.1007/978-981-19-9768-6_41.

Napitupulu G., Nagi A., Putri M.R. and Radjawane I.M.; 2023: *The one-dimensional (1D) numerical model: an application to oxygen diffusion in Mitochondria Cell.* ComTech: Comput. Math. Eng. Appl., 14, 101-118, doi: 10.21512/comtech.v14i2.9705.

Napitupulu G., Farihah R.A., Manik H.M., Larasati O.D.D., Napitupulu M., Bernawis L.I., Radjawane I. and Kusmanto E.; 2024a: *Zooplankton distribution from backscatter data of ADCP instrument in west Sumatra waters.* Bull. Mar. Geol., 39, 84-95, doi: 10.32693/bomg.39.2.2024.871.

Napitupulu G., Lukman A.A., Hatmaja R.B., Kartadikaria A.R., Radjawane I.M., Millina A.V., Apdillah Akbar M. and Napitupulu M.; 2024b: *Respon Singkat Konsentrasi Klorofil-a Terhadap Perubahan Arus Eddy Permukaan di Wilayah Perairan Teluk Tolo dan Sekitarnya.* J. Geol. Kelautan, 22, 26-40, doi: 10.32693/jgk.22.1.2024.877. (in Indonesian)

Napitupulu G., Zulfikar R., Yulianti K.K., Sinuraya D.E., Waryatno N.F.P. and Fekranie N.A.; 2024c: *Spatiotemporal variation of Particulate Matter (PM) 2.5 concentration in the Indonesian maritime continent.* Malaysian J. Trop. Geogr. (MJTG), 50, 1-17, doi: 10.5067/KLICLTZ8EM9D.

Napitupulu G., Fekranie N.A., Millina A.V., Putri M.R., Kartadikaria A.R., Setiawan A., Hatmaja R.B. and Fajary F.R.; 2025a: *Seasonal variability of surface Heat Transport in the Banda Sea.* Thalassas: an Int. J. Mar. Sci., 41, 105, doi: 10.1007/s41208-025-00840-4.

Napitupulu G., Nagi A., Nurdjaman S., Radjawane I.M., Rachmayani R., Ramadhan M.R., Nasution M.I., Habibullah A.D. and Kelvin F.M.; 2025b: *Impact of marine heatwaves and cold spells on coral reef ecosystem in a tropical region: a case study of Lombok Waters, Indonesia.* Mar. Syst. Ocean Tech., 20, 16, doi: 10.1007/s40868-024-00160-x.

Nezlin N.P., Sutula M.A., Stumpf R.P. and Sengupta A.; 2012: *Phytoplankton blooms detected by SeaWiFS along the central and southern California coast.* J. Geoph. Res., 117, 7004, doi: 10.1029/2011JC007773.

Nicholls N.; 1988: *El Niño - Southern oscillation and rainfall variability.* J. Clim., 1, 418-421, doi.org/10.1175/1520-0442(1988)001<0418:ENOARV>2.0.CO;2.

Nurfitri S., Basit A., Putri M.R., Pätsch J. and Pohlmann, T.; 2020: *A Lagrangian study of upwelled waters in the Northern Arafura Sea.* IOP Conf. Ser., Earth Environ. Sci., 618, doi: 10.1088/1755-1315/618/1/012022.

Pierella-Karlusich J.J., Ibarbalz F.M. and Bowler C.; 2020: *Phytoplankton in the Tara Ocean.* Ann. Rev. Mar. Sci., 12, 233-265, doi: 10.1146/ANNUREV-MARINE-010419-010706/1.

Quan W. and Chen J.; 2023: *Algal biological features viewed in satellite observations: a case study of the Bohai Sea.* Remote Sens., 15, 4999, doi: 10.3390/rs15204999.

Racault M.F., Sathyendranath S., Brewin R.J., Raitsos D.E., Jackson T. and Platt T.; 2017: *Impact of El Niño variability on oceanic phytoplankton.* Front. Mar. Sci., 4, 133, doi: 10.3389/fmars.2017.00133.

Radjawane I.M., Saleh E., Napitupulu G., Abdillah M.R. and Hassan M.A.M.; 2024a: *Seasonal variability of sea surface chlorophyll-a at west Borneo Island.* The Indonesian. J. Geogr., 56, 70-81, doi: 10.22146/ijg.87713.

Radjawane I.M., Yusarita A., Kuswardani A.R.T.D. and Napitupulu G.; 2024b: *Pengaruh Sirkulasi Arus Geostropik dan Ageostropik Terhadap Upwelling di Perairan Selatan Jawa.* Buletin Oseanografi Marina, 13, 448-463, doi: 10.14710/buloma.v13i3.62368 (in Indonesian).

Rashid I.U., Abid M.A., Almazroui M., Kucharski F., Hanif M., Ali S. and Ismail M.; 2022: *Early summer surface air temperature variability over Pakistan and the role of El Niño–Southern Oscillation teleconnections.* International Journal of Climatology, 42(11), 5768-5784, doi: 10.1002/joc.7560.

Resosudarmo B.P., Napitupulu L. and Campbell D.; 2009: *8 Illegal fishing in the Arafura Sea.* In: Resosudarmo B.P. and Jotzo F. (eds), Working with Nature against Poverty: Development, Resources and the Environment in eastern Indonesia, ISEAS Publishing Singapore, pp. 178-200, doi: 10.1355/9789812309600-014"10.1355/9789812309600-014.

Setiawan R.Y., Wirasatriya A., Hernawan U., Leung S. and Iskandar I.; 2020: *Spatio-temporal variability of surface chlorophyll-a in the Halmahera Sea and its relation to ENSO and the Indian Ocean Dipole.* Int. J. Remote Sens., 41, 284-299, doi: 10.1080/01431161.2019.1641244.

Sinuraya D.E., Fitriani R., Fajary F.R. and Napitupulu G.; 2023: *Influence of madden julian oscillation based on rainfall on variability of particulate matter 2.5 concentration in Indonesian maritime continent.* In: Proc. International Conference on Radioscience, Equatorial Atmospheric Science and Environment, Springer Nature, Singapore, Vol. 305, pp. 55-64, doi: 10.1007/978-981-97-0740-9_6.

Suryadarma M.W., Okgareta D., Latuapo N.H. and Atmadipoera A.S.; 2023: *Seasonal variation of some oceanographic parameters in the Arafura Sea - Gulf of Carpentaria.* IOP Conf. Ser., Earth Environ. Sci., 1137, 012011, doi: 10.1088/1755-1315/1137/1/012011.

Susanto R.D., Gordon A.L. and Zheng Q.; 2001: *Upwelling along the coasts of Java and Sumatra and its relation to ENSO.* Geophys. Res. Lett., 28, 1599-1602, doi: 10.1029/2000GL011844.

Tirtadanu T., Amri K., Makmun A., Priatna A., Pane A.R.P., Wagiyo K. and Yusuf H.N.; 2022: *Shrimps distribution and their relationship to the environmental variables in Arafura Sea.* IOP Conf. Ser., Earth Environ. Sci., 1119, 012003, doi: 10.1088/1755-1315/1119/1/012003.

Uitz J., Claustre H., Morel A. and Hooker S.B.; 2006: *Vertical distribution of phytoplankton communities in open ocean: an assessment based on surface chlorophyll.* J. Geophys. Res. Oceans, 111, 8005, doi: 10.1029/2005JC003207.

Utama F.G., Atmadipoera A.S., Purba M., Sudjono E.H. and Zuraida R.; 2017: *Analysis of upwelling event in southern Makassar Strait.* IOP Conf. Ser., Earth Environ. Sci., 54, 012085, doi: 10.1088/1755-1315/54/1/012085.

Von Schuckmann K., Le Traon P.Y., Alvarez-Fanjul E., Axell L., Balmaseda M., Breivik L-A., Brewin R.J.W., Bricaud C., Drevillon M., Drillet Y., Dubois C., Embury O., Etienne H., Sotillo M.G., Garric G., Gasparin F., Gutknecht E., Guinehut S., Hernandez F., Juza M., Karlson B., Korres G., Legeais J.-F., Legeais J.-F., Levier B., Lien V.S., Morrow R., Notarstefano G., Parent L., Pascual A., Pérez-Gómez B., Perruche C., Pinardi N., Pisano A., Poulain P.-M., Pujol I.M., Raj R.P., Raudsepp U., Roquet H., Samuelsen A., Sathyendranath S., She J., Simoncelli S., Solidoro C., Tinker J., Tintoré J., Viktorsson L., Ablain M., Almroth-Rosell E., Bonaduce A., Clementi E., Cossarini G., Dagneaux Q., Desportes C., Dye S., Fratianni C., Good S., Greiner E., Gourrion J., Hamon M., Holt J., Hyder P., Kennedy J., Manzano-Muñoz F., Melet A., Meyssignac B., Mulet S., Nardelli B.B., O'Dea E., Olason E., Paulmier A., Pérez-González I., Reid R., Racault M.-F., Raitsos D.E., Ramos A., Sykes P., Szekely T. and Verbrugge N.; 2016: *The Copernicus marine environment monitoring service ocean state report.* J. Oper. Oceanogr., 9, s235-s320, doi: 10.1080/1755876X.2016.1273446.

Vos K., Splinter K.D., Palomar-Vázquez J., Pardo-Pascual J.E., Almonacid-Caballer J., Cabezas-Rabadán C. and Vitousek S.; 2023: *Benchmarking satellite-derived shoreline mapping algorithms.* Commun. Earth Environ., 4, 345, doi: 10.1038/s43247-023-01001-2.

Wang D., Fang G., Jiang S., Xu Q., Wang G., Wei Z. and Xu T.; 2022: *Satellite-detected phytoplankton blooms in the Japan/East Sea during the past two decades: magnitude and timing.* Front. Mar. Sci., 9, 1065066, doi: 10.3389/fmars.2022.1065066.

Wang Y., Jiang H., Jin J., Zhang X., Lu X. and Wang Y.; 2015: *Spatial-temporal variations of chlorophyll-a in the adjacent sea area of the Yangtze River estuary influenced by Yangtze River discharge*. Int. J. Environ. Res. Publ. Health, 12, 5420-5438, doi: 10.3390/IJERPH120505420.

Welliken M.A., Melmambessy E.H.P., Merly S.L., Pangaribuan R.D., Lantang B., Hutabarat J. and Wirasatriya A.; 2018: *Variability chlorophyll-a and sea surface temperature as the fishing ground basis of Mackerel fish in the Arafura Sea.* In: Proc. 3rd International Conference on Energy, Environmental and Information, E3S Web of Conferences, Vol. 73, 04004, doi: 10.1051/E3SCONF/20187304004.

Wiafe G. and Nyadjro E.S.; 2015: *Satellite observations of upwelling in the Gulf of Guinea.* IEEE Geosci. Remote Sens. Lett., 12, 1066-1070, doi: 10.1109/LGRS.2014.2379474.

Willey J.D., Paerl H.W. and Go M.; 1999: *Impact of rainwater hydrogen peroxide on chlorophyll a content of surface Gulf Stream seawater off North Carolina, USA.* Mar. Ecol. Progr. Ser., 178, 145-150, doi: 10.3354/MEPS178145.

Xu M., Wang Y., Feng Z. and Wu H.; 2024: *Rapid variations of phytoplankton blooms and their dynamics off the Changjiang River estuary.* Front. Mar. Sci., 11, 1345940, doi: 10.3389/fmars.2024.1345940.

Xu T., Wei Z., Li S., Susanto R.D., Radiarta N., Yuan C. and Trenggono M.; 2021: *Satellite-observed multi-scale variability of sea surface chlorophyll-a concentration along the south coast of the Sumatra-Java islands.* Remote Sens., 13, 2817, doi: 10.3390/rs13142817.

Yuliardi A.Y., Napitupulu G., Rachman H.A., Prayogi H., Joesidawati M.I. and Prasita V.D.; 2025: *Spatiotemporal analysis of sea surface temperature and chlorophyll-a variability under ENSO-IOD influence in the southern Madura Strait, Indonesia.* Vietnam J. Earth Sci., 47, 546-564, doi: 10.15625/2615-9783/23665.

Zhang C., Liu Y., Chen X. and Gao Y.; 2022: *Estimation of suspended sediment concentration in the yangtze main stream based on sentinel-2 MSI data.* Remote Sens., 14, 4446, doi: 10.3390/rs14184446.

Corresponding author: Gandhi Napitupulu
Bandung Institute of Technology: Bandung, West Java Indonesia
Kebonturi Street, Arjawinangun Cirebon Regency, Bandung, West Java 45162, Indonesia
Phone: +62 823 6202 4912; e-mail: gandhinapitupulu88@gmail.com